2009-01-01

Observed Superspin-Glass behavior in Ni0.5Zn0.5Fe2O4 Nanoparticles

Antony Adair
University of Texas at El Paso, ahadair@miners.utep.edu

OBSERVED SUPER-SPIN GLASS BEHAVIOR IN $Ni_{0.5}Zn_{0.5}Fe_2O_4$ NANOPARTICLES

ANTONY ADAIR

Department of Physics

APPROVED:

_____
Cristian E. Botez, Ph.D., Chair

_____
Russell R. Chianelli, Ph.D.

_____
Marian-Mihae Manciu**,** Ph.D.

_____
Patricia D. Witherspoon, Ph.D.
Dean of the Graduate School.

OBSERVED SUPER-SPIN GLASS BEHAVIOR IN $Ni_{0.5}Zn_{0.5}Fe_2O_4$ NANOPARTICLES

by

ANTONY ADAIR

THESIS

Presented to the Faculty of the Graduate School of

The University of Texas at El Paso

in Partial Fulfillment

of the Requirements

for the Degree of

MASTER OF SCIENCE

Department of Physics

THE UNIVERSITY OF TEXAS AT EL PASO

August 2009

Acknowledgements

It is difficult to overstate my gratitude for my mentor, Dr. Cristian Botez, with his enthusiasm, his inspiration, and his great efforts to explain things clearly and simply. He has continuously provided encouragement, sound advice, good teaching, and lots of good ideas. I would also like to Thank Dr. Ronald Tackett for all the time and effort he took out of his busy schedule help me with this thesis. Without Dr. Tackett's guidance and feedback, I doubt this thesis would have been able to be completed.

I would like to acknowledge the Minority Access to Research Careers, Undergraduate Student Training in Academic Research (MARC U-STAR) program for its all its support and the wonderful learning opportunities it provided me as an undergraduate. I would also like to thank the Gateway program, from where I received my first taste of being a real scientist as well as an extensive amount of laboratory training.

I would like to thank Dr. Russell Chianelli for all the wonderful opportunities he has given me throughout the years, as well as being an excellent role model of a successful researcher and businessman. A special gratitude is due to Dr. Keith Pannell director of the UTEP MARC U-STAR program, for all his encouragement, teaching, as well as providing a venue where likeminded future scientists can come together and actively discuss important scientific issues.

Finally, I would like to express the upmost gratitude to Dr. Cristian Botez, Dr. Russell Chianelli and Dr. Marian-Mihae Manciu for taking time out of their busy schedules to serve on my thesis committee.

Abstract

OBSERVED SUPER-SPIN GLASS BEHAVIOR IN $Ni_{.5}Zn_{.5}Fe_2O_4$ NANOPARTICLES

M.S. candidate: Antony Adair

Advisor: Dr. Cristian E. Botez

In this investigation we seek to identify the magnetic behavior of $Ni_{0.5}Zn_{0.5}Fe_2O_4$ nanoparticles though AC-susceptibility and DC-magnetization measurements. Powder x-ray diffraction was performed to determine the purity and average diameter (<D> ˜ 9nm) of the particles. Aditionally, structure was confirmed by comparison through the International Centre for Diffraction Data's Powder Diffraction File [52] (PDF # 08-0234).

Zero-field cooled and field cooled DC magnetization measurements (bifurcation and blocking temperature), as well as M(H) hysteresis (below and above the blocking temperature) lead us to initially suggest that the material may in fact be superparamagnetic. However, further investigation of the real AC susceptibility through typical magnetic models (Néel- Arrhenius, Vogel Fulcher), suggest an influence from interparticle interactions on the overall magnetic behavior of the system. In addition, the relative variation of the blocking temperature per frequency decade was 0.032 within the range commonly associated with spin glass behavior (0.007 - .05) [75,76].

Further investigation leads us to conclude that the in-phase component of the AC susceptibility is well described by the critical dynamics of the power law, commonly associated with spin-glass behavior. Our parameters were well within observed spin-glass range, showing a critical dynamic exponent zv=10 (range 8-10) and attempt frequency 10^{11}Hz (range 10^{11} -

10^{13}Hz) [77]. The transition temperatures DC field dependence was found to follow the AT line (commonly associated with glassy behavior) and showed a zero field freezing temperature consistent with that found from the power law fit, further evidencing super-spin-glass behavior [79]. Additionally, the out-of-phase component of the AC susceptibility was probed for dynamic scaling behavior (associated with spin-glass like systems). The data produced parameters (β=1.0) in perfect agreement with already established values for spin-glass systems [80]. Furthermore thermo-remnant magnetization (TMR) measurements lead to a peak at the wait temperature, this peak has been used previously to differentiate between super-spin glasses and superparamagnets. Throughout our investigation, all magnetization experiments seem to point to the likelihood of super spin-glass behavior in the $Ni_{0.5}Zn_{0.5}Fe_2O_4$ nanoparticle system.

Table of Contents

List of Figures

Page

Chapter 1: Introduction

Currently, nickel zinc ferrites are used for their magnetic properties in the modern electronics industry, due to their high electrical resistivity. These high electrical resistivities imply very low eddy current losses, only significant at higher electromagnetic field frequencies. In addition nickel zinc ferrites exhibit many other properties that make them valuable to the electronic industry including, high mechanical strength, high values of saturation magnetization/magnetic permeability, excellent chemical stability, and low coercivities/dielectric losses [1].

The electronics industry is turning to nanosized nickel zinc ferrite to reduce the energy losses commonly associated with bulk powders. Furthermore nickel zinc ferrite nanoparticles are prime candidates for the changing face of electronics, as more and more electronic applications require materials be pressed into larger shapes with near theoretical density (difficult to obtain if the particles have a wide size distribution) [2].

Evidently there are a large number of potential applications of nickel zinc ferrite nanoparticles, as well as magnetic nanoparticles in general, including the electronic/computer industry and biomedical sciences. Applications aside, the study and classification of magnetic nanoparticles, spinel ferrites in particular, is of great importance to our understanding of material magnetization in general. It will only be through numerous studies of all types of spinel ferrites that we will be able to use these materials to the fullest.

In this study we present our investigation of the magnetic behavior of nanosized spinel ferrite $Ni_{0.5}Zn_{0.5}Fe_2O_4$, though means of dc and ac magnetic susceptibility as well as powder X-ray diffraction (XRD) measurements. In addition to the geometric structure of the sample, our study produces a wide array of evidence that shows superspin-glass behavior in this material.

1.1 Why Magnetic Nanoparticles?

Magnetic nanoparticles have been found to exhibit may interesting properties, most notably, properties that appear to be size induced. Consequently, many unique and unexpected magnetic behaviors arise in magnetic nanoparticles. Perhaps most notably is the well known below some critical size.

Over the last few decades the dynamics of how magnetic nanoparticles interact has been a subject of extensive research [3-5]. While numerous work has been done on magnetic nanoparticle systems simply to increase our basic understanding of magnetism, the recent surge in magnetic nanoparticle research has primarily been motivated by two main industries, the electrical industry/computer sciences [6-8], and the biosciences [9,10]. In addition due to recent breakthroughs involved in synthesis, as well as the United States government's strong recognition of nanoparticle importance, magnetic nanoparticles make an optimal candidate for university research.

In the biosciences, a wide variety of applications of magnetic nanoparticles has been envisaged, including magnetic hyperthermia (cancer treatment) [11], and magnetic immunoassay [12] (using magnetic beads for diagnosis). The great potential of using magnetic nanoparticles in the biosciences stems from the presumed ability to control key magnetic properties, chemical binding properties, reliable retrieval or dispersion mechanisms which magnetic particles provide, as well as the ability to locate said particles in a unobtrusive fashion (magnetic imaging techniques).

In the electronics industry and computer sciences, the main driving force is that of producing higher density magnetic storage media [13]. The magnetic data storage industries are constantly seeking to improve their technologies, making faster and smaller data storage

materials. Because there are some presumed limitations (mutual dipolar interactions, superparamagnetic limit) to making data storage devices in the current manner, much interest has been generated by the claims that there are ways to produce materials around said "limits", (ex. arrays of single-domain magnetic nanoparticles may lead to ultrahigh density magnetic recording media [14]).

Magnetic nanoparticles are practical to work with as there has been great advances in their synthesis, allowing for easier and more economical production. Accordingly, there have been extensive chemical procedures developed (*rf* sputtering [15], chemical synthesis [14]) to precisely tailor magnetic nanoparticles for specific composition and size. In addition, nanoparticles research in the United States is generally cast in a favorable light due in part to programs such as The National Nanotechnology Initiative, which provides generous public funding for nanoparticle research [16].

Ultimately it will be our understanding of the different types of magnetic behavior present in magnetic nanoparticles (transitions, relaxations, reversal dynamics [3]) and how these behaviors arise from the chemical composition that lead us to manipulate such systems for our benefit. Therefore, numerous theories and studies have been developed, dedicated to explain, classify and hypothesize the complex inner workings of magnetic nanoparticles. It is only through work such as this (our own work included) that progress is made towards the ultimate goal of the field, a completely developed coherent model explaining the behavior of magnetic nanoparticles.

1.2 Why Zinc Doped Nickel Ferrite?

For the past few decades, much research has been dedicated to the study of magnetic nanoparticles, especially regarding the direct influence of size effects on the behavior of the

whole (the system composted of many nanoparticles). Although, perhaps more fundamentally important, is the area of research concerning the effect of the whole in response to changes within the nanoparticles crystal structure/composition. In particular, our study (like various others) seeks to correlate how changes in the crystal structure/composition of a nanoparticle system influences the magnetic properties of the system as a whole. Therefore we choose to study a mixed-oxide nanoparticle ensemble, as it is known that most properties that arise from mixed-oxide nanoparticles depend not only directly on the size but also through the influence of the crystalline structure/composition of the nanoparticles themselves.

Our baseline (undoped) mixed-oxide nanoparticle of choice was nickel ferrite ($NiFe_2O_4$) for several reasons. First of all, nickel ferrite belongs to a particular group of materials structures called spinel ferrites. Magnetic spinel ferrites can typically be constructed on the nanoscale range without requiring any extreme laboratory conditions. Furthermore, spinel ferrite nanoparticles allow for an easy geometric understanding of the structure upon doping. The effect of doping a spinel ferrite can usually be directly understood geometrically, and hence allows for direct correlation of the samples crystalline structure/composition with the nanoparticle systems magnetic behavior. Consequently, spinel ferrites offer opportunities for the understanding and fine-tuning of particles magnetic properties through chemical manipulations.

In addition magnetic spinel ferrite nanoparticle systems have been extensively studied throughout the last decade [17-19]. Much attention has been focused on the preparation and characterization of transition metal spinel ferrites of the form MFe_2O_4 (metal M = Co, Mg, Mn, Zn, etc.) [20-25], making for ample scientific literature for comparison and conjecture. While a great deal of work has been done on spinel ferrite nanoparticles, and every type of possible

magnetic behavior has been observed, there is yet to be a complete theory to categorize their magnetic behavior in full.

We decided to use zinc as the dopant for this experiment as previous studies [26] have indicated that adding Zn^{2+} ions to bulk spinel ferrites has a strong effect on their magnetic properties (although surprisingly enough Zn^{2+} is non-magnetic). The combination of the baseline nickel ferrite behavior and the supposed magnetic change that may occur upon doping, suggest that any induced magnetic behavior would be relatively easy to observe. Furthermore, should other nanoparticles exhibit changes in magnetic properties upon Zn-doping, then Zn-doping might be used in general to control key properties that are specific to nanoparticles.

Chapter 2: Theoretical Background

2.1 Structure

In our investigations, we effectively studied nano-sized zinc doped nickel ferrite, synthesizing the non-stoichiometric $Ni_{0.5}$ $Zn_{0.5}Fe_2O_4$. This particular type of chemical system belongs to a group of crystal compounds classified as spinel ferrites, which are in turn classified as spinels. The fact that our material is classified as nano-sized is merely an indication of the average particle size of our spinels.

2.1.1 Nanoparticles

A nanomaterial is defined as a material with at least one spatial dimension in the nanoscale range (10^{-9} meters). Nanoparticles usually behave as a whole unit in terms of their transport and various other properties. Nanoparticle classification is generally done in terms of average diameter, with "fine" nanoparticles between 100 and 2500 nanometers, and "ultrafine" sized between 1 and 100 nanometers.

Nanoparticle research is an active area of scientific research due to the variety of interesting properties including magnetic, optic, and size related [27] phenomena. Nanoparticle research is of great interest because they effetely bridge the gap between the molecular scale physics and bulk materials physics.

Due to the plethora of interesting phenomena present in nanoparticles, they have potential applications in computational, optical, biomedical, and electrical sciences. Nanoparticle research has already foreshadowed application as magnetic storage media and in the biosciences.

2.1.2 Spinels

Specifically spinel is $MgAl_2O_4$. An entire group of materials, classified as spinels are those with crystal structures of the form, $(A^{2+})(B^{3+})_2(O^{2-})_4$ [28]. Although typically oxides, there

are other structures classified as spinels in which the oxygen is replaced by another chalcogenide. Spinels form a cubic closed-packed lattice with one octahedral and two tetrahedral sites per molecule (Fig 2.1, 2.4). The Octahedral points are generally larger the tetrahedral points.

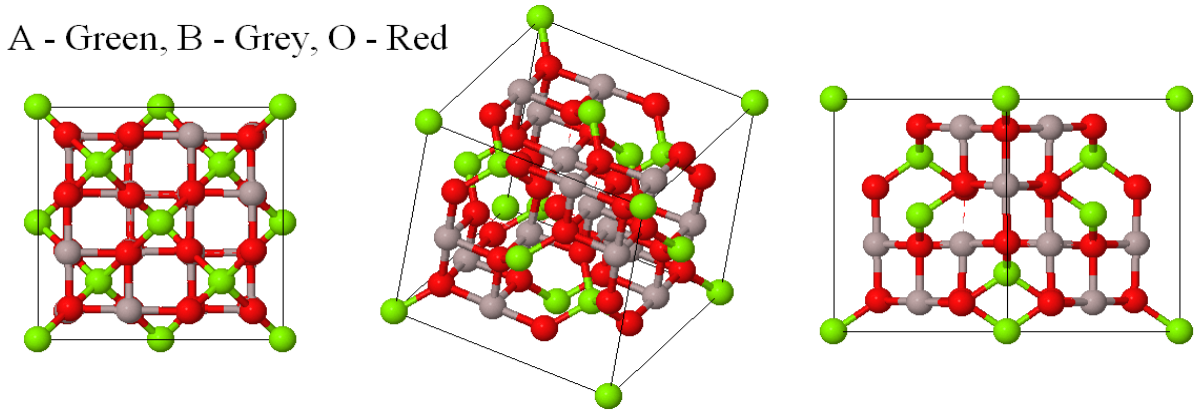

Figure 2.1: Normal Spinel

In normal spinels (such as $MgAl_2O_4$), the B^{3+} ions occupy the octahedral sites (Fig 2.3), whereas the A^{2+} ions occupy the tetrahedral sites (Fig 2.2). This arrangement maximizes the lattice energy if the ions are similar in size. Since there is essentially a 2:1 ratio of the tetrahedra to octrahedra sites, and a ½:1/8 ratio of respected site filling, this directly implies there is twice as many filled octahedra as tetrahedra. In addition the spinel formula implies this same 2:1 ratio of the B and A anions, implying it is possible to fill all the octahedra with B (trivalent) atoms and the tetrahedra with A (divalent) atoms (normal spinel structure).

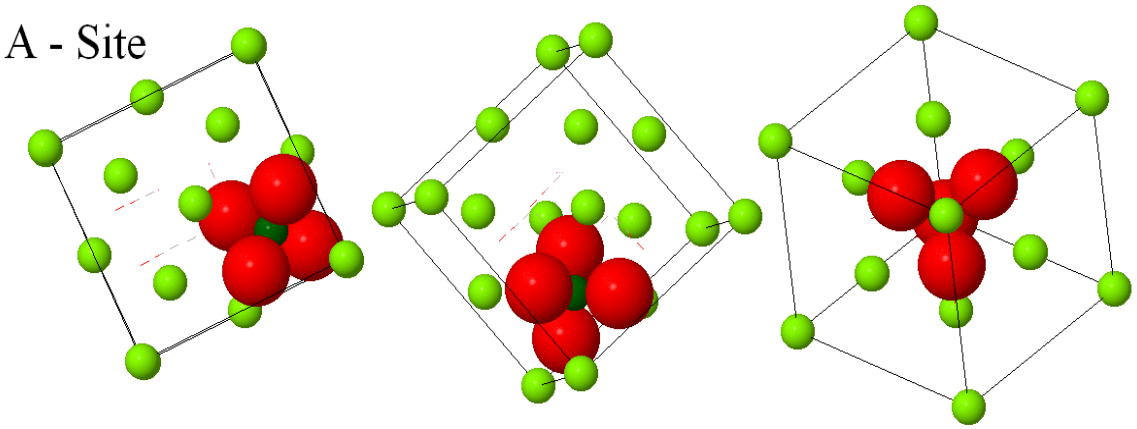

Figure 2.2: Normal Spinel – (A – Site)

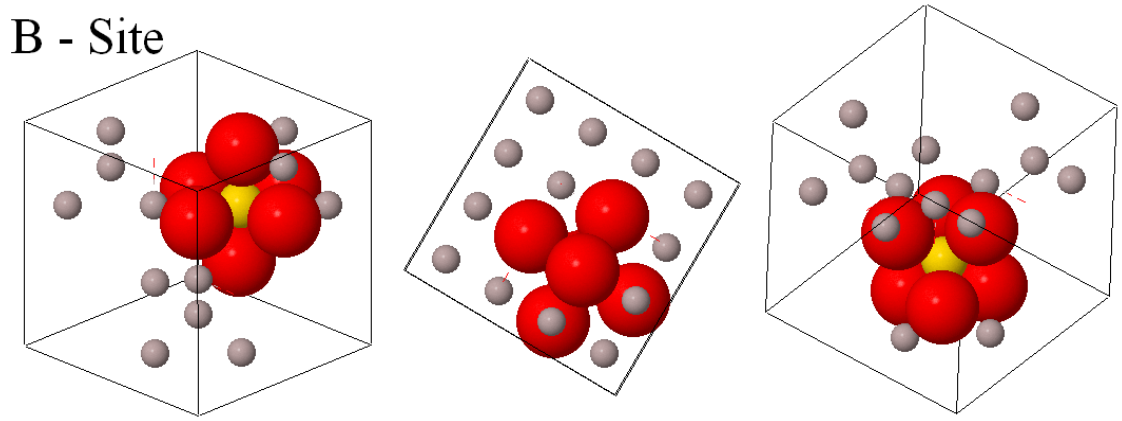

Figure 2.3: Normal Spinel – (B – Site)

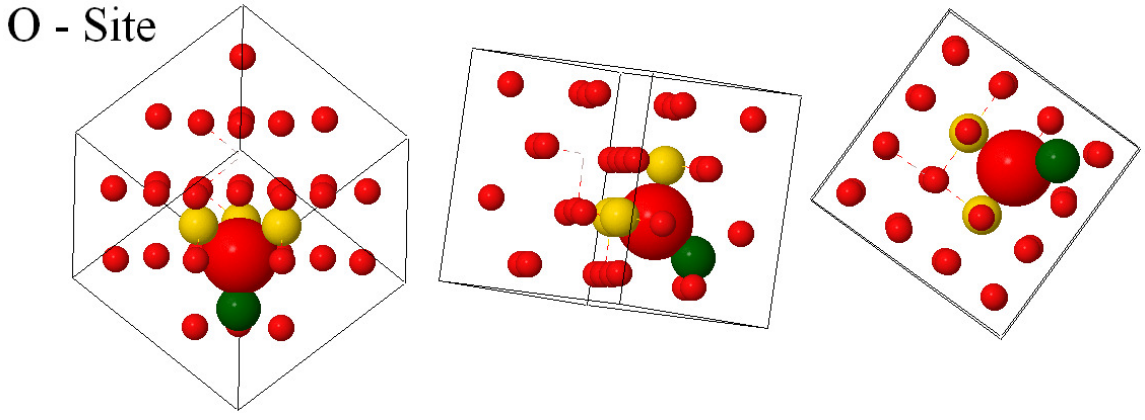

Figure 2.4: Normal Spinel – (O – Site)

An inverse spinel (such as $FeCr_2O_4$) occurs when the roles of the B and A anions are reversed. By filling the tetrahedral sites with only B^{3+} anions, some octahedral sites will be left

empty. Since there is a 2:1 ratio of octrahedra to tetrahedra and B^{3+} to A^{2+} anions, the possible ways to arrange such a system are limited. The only way to accomplish filling only the tetrahedra with B^{3+} anions, is by filling half the octrahedra with A^{2+} anions, the tetrahedra taking half of the B^{3+} anions, and the remaining B^{3+} anions filling vacant octrahedra sites (inverse spinel).

In addition to normal spinels and inverse spinels there are several other classifications all relating to the placement of the A and B ions in the octahedral and tetrahedral sites. In reality, most spinel structures are somewhere in-between the normal and inverse structure. Numerous theories involving atomic orbitals have been developed to account for the different site ordering that can occur in spinels [29].

2.1.3 Ferrites

A spinel ferrite (or simply ferrite) is a group of spinels in which the cations are transition metals (one of them being iron), and the anion is oxygen. Spinel ferrites are typically magnetic ceramics in nature, and are commonly used in the electronic/computer industry and to construct permanent magnets.

Ferrites are usually classified into two groups in reference to there coercivity of magnetism, soft (low coercivity) and hard (high coercivity). Due to their comparatively low losses at high frequencies, soft ferrites are often used in the cores of inductors, and as RF transformers. Common soft ferrites used in the industry today usually contain nickel, zinc, or manganese. Hard ferrites have a high magnetic coercivity and high remnant magnetization, as well as a high magnetic permeability. Hard ferrites are typically cheap to make, and are subsequently used as permanent household magnets (refrigerator magnets, etc). Common hard ferrites used in industry today are typically composed of iron , barium, or strontium oxides.

Additionally, hard ferrites are known to still conduct magnetic flux at magnetic saturation, often enabling them to store stronger magnetic fields than iron [1].

2.1.2 Zinc Doped Nickel Ferrite

Nickel ferrite occurs in nanoparticle spinel clusters, and has chemical formula $(Ni)(Fe^{3+})_2O_4$. Nickel Ferrite occurs naturally within the earth as a black mineral, and is studied extensively by earth scientist and geologist under the name Trevorite. Nickel Ferrite is an ideal spinel, as its properties make it an ideal representation of the spinel group as a whole.

Zinc doped nickel ferrite has the same structure as Nickel ferrite, the exception being that some of the Ni^{2+} ions have been replaced by Zn^{2+} ions. There is strong evidence that indicates adding Zn^{2+} ions to bulk spinel ferrites has a strong effect on their magnetic properties, even though Zn^{2+} ions are non-magnetic [26]. Because zinc doped nickel ferrite is non-stoichiometric, it is not straight forward as to exactly what anion sites are replaced physically. In this experiment, $Ni_{.5}\ Zn_{.5}Fe_2O_4$ was produced in a powder form, and x-ray diffraction measurements were carried out to confirm phase purity.

2.2 Magnetization

Because we are seeking to describe the magnetic behavior of nickel zinc ferrite nanoparticles, a summary of the basic types of known magnetic behavior is appropriate. In addition a brief explanation of the cause of magnetization within a material is touched upon.

2.2.1 Origin of Magnetism

The origins of magnetism lie in electrodynamics and quantum mechanics. It is the combination of an electrons orbital angular momentum and intrinsic spin that form a magnetic dipole moment resulting in a magnetic field. While theoretically magnetic fields are similarly generated by nucleons (or any other particle with electric charge), there net contribution is so

insignificant that it can usually be ignored. The different magnetic fields generated within a material simply obey the rule of superposition, subsequently giving an object its net magnetic field and magnetic behavior [30].

From basic electrodynamics it is known that objects that generate magnetic fields are also affected by magnetic fields. Consequently, within a material, every particle generating a magnetic field is subsequently influencing and being influenced magnetically by every other particle generating a magnetic field. Hence an extremely delicate complicated dynamic magnetic system can be produced in a material.

To better understand magnetic behavior of a material is useful to take the simplest case, two dipoles in close proximity. Using basic electromagnetism, we would expect the two dipoles to align in opposite directions almost always, however when you take into account the Pauli Exclusion Principle [31] (for the electrons) you see this does not have to be the case. In fact if the two dipoles are aligned parallel, it would effectively reduce the energy of their electrostatic interaction compared with that of oppositely aligned dipoles. This difference in energy is called the exchange energy and can be fully described by exchange interactions.

The exchange interaction is a quantum mechanical effect that describes the change of the expectation value of energy or distance between identical particles due to wave functions overlap. This phenomenon was independently discovered by two of the fathers of quantum mechanics, Heisenberg [32] and Dirac [33]. This quantum mechanical effect is the primary cause of the ordering of atomic magnetic moments in magnetic solids.

The first parameter that must be addressed when dealing with magnetic materials is the material's magnetization. This quantity is proportional to the magnetic moment of the particle or

collection of particles in question. The magnetic moment is a measure of the strength and direction of the magnetization of a material.

Magnetic susceptibility is a dimensionless parameter associated with the degree of magnetization of a material that responds to an applied magnetic field. In its most basic form magnetic susceptibility is:

$$\chi = \partial \mathbf{M} / \partial \mathbf{H} \tag{1}$$

Frequently, materials are classified according to their magnetic susceptibility. A diamagnetic is a material that has a negative susceptibility, i.e. the materials magnetization opposes any applied external magnetization. A paramagnet has a positive magnetic susceptibility and its magnetization follows the applied external field linearly.

In the absence of an external magnetic field the individual moments of a diamagnetic or paramagnet are thermally disordered and pointing in random directions, thus leading to an overall zero net magnetization.

While diamagnetism and paramagnetism explain a great deal of magnetic systems, they don not take into account interactions between atomic moments. A ferromagnet has strong enough inter-moment interactions to overcome this thermal disordering below a certain temperature (transition temperature). The interactions in a ferromagnet favor parallel magnetic alignment. Magnetic domains will typically form in ferromagnets as the energy required to maintain completely parallel alignment throughout the whole material is overtaken by distance. Consequently when the material is in an external magnetic field the domains which were already parallel to the field will be seen to grow, while those less aligned with the field will shrink.

2.2.2 Magnetic Domains

Considering the multitude of ions in a material, the exchange energy advantage may be overtaken by the classical electrodynamics tendency of dipoles to anti-align, creating a non-net-magnetized material. In such cases, the material is generally said to be made of different magnetic "domains" [34]. Each of these domains describes a region in which there is a uniform magnetization, as all moments are aligned in the domain. The separation between the domains is referred to as the domain wall.

As an external filed is applied, the domains which were already parallel are seen to grow in size (Fig 2.5). All domains can generally be aligned if a strong external magnetic field is applied, in such case they are all aligned parallel to the external magnetic field.

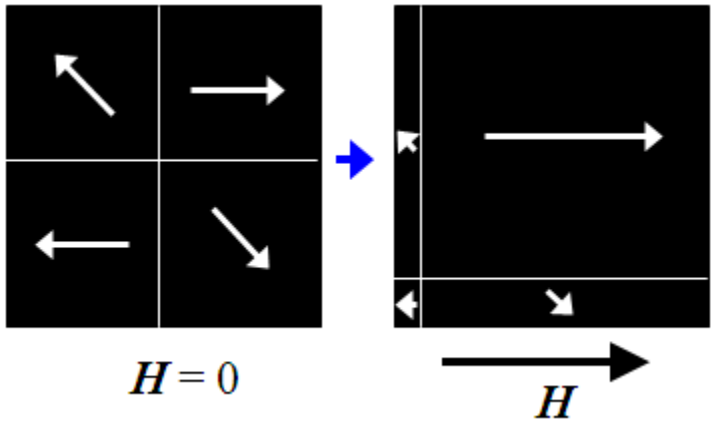

Figure 2.5: Growth of Magnetic Domains

2.2.3 Ferromagnetism

In ferromagnetic materials, magnetic moments of neighboring atoms align, resulting in very large internal magnetic fields, ordered magnetic structure, and consequently, magnetic domains. In effect, it is magnetic domain dynamics that govern ferromagnetic behavior.

Ferromagnetism is the form of magnetism known to most civilizations since antiquity. Good examples of ferromagnetic objects are refrigerator magnets, horse shoe magnets and bar magnets. Historically, a ferromagnet is defined as an object that becomes magnetized upon application of an external magnetic field, and remains magnetized after the field is removed. The standard modern definition of a ferromagnet also requires that all its ions add a positive contribution to the net magnetization (total alignment), as opposed to a ferrimagnet, in which some magnetic ions subtract from the net magnetization (partial anti-alignment), or an anti-ferromagnet, in which enough ions subtract from the net magnetization so that the total magnetic field is zero (anti-alignment) [35] (Fig 2.6). Although often all these terms are used interchangeably or referred to as ferromagnets.

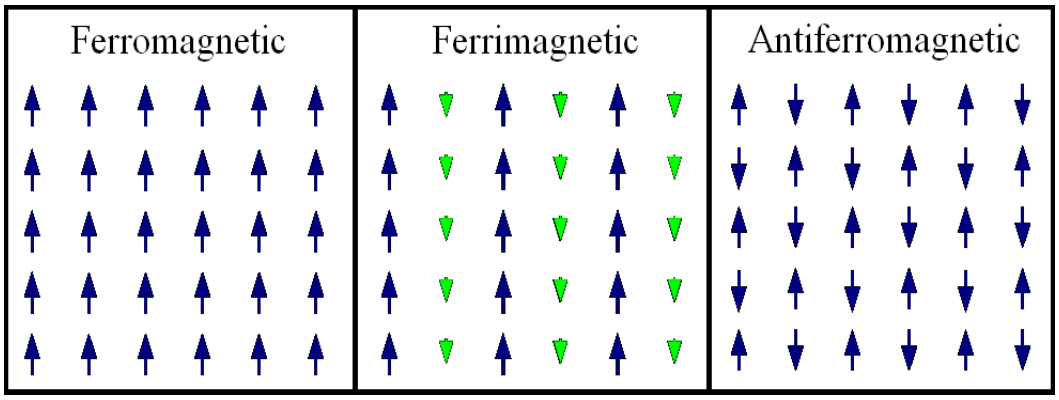

Figure 2.6: Ferromagnetic, Ferromagnetic and Ant ferromagnetic behavior

Ferromagnetism explains why application of a magnetic field to a non-magnetized piece of iron, causes it to become magnetized, a “permanent” magnet. Materials magnetized in this fashion aren’t in their minimized energy configuration though so it reasons that eventually they will revert to non-magnetized states. The time this process takes could be seconds to millions of years depending on the specific material.

2.2.4 Paramagnetism

Paramagnetism is another type of basic magnetism known to most. A material is paramagnetic if all its dipoles align in an external magnetic field (parallel to the field), yet without the external magnetic field the material forms no domains, and exhibits no net-magnetism.

In terms of energy, a paramagnet occurs when there is sufficient thermal energy to overcome the interaction energy between dipoles (in the absence of an external magnetic field). Hence there is no parallel ordering or ordering into domains, as in a ferromagnet, because the dipoles do not interact with each other. All dipoles are continuously moving in a random fashion independent of each other, due to thermal energy. If by chance the dipoles do interact and manage to form some long range order or domains (as in some materials), the material would be a ferromagnet by definition.

2.2.5 Superparamagnetism

An interesting phenomena occurs in ferromagnetic materials in which the size of the particles approaches some critical size (usually nanoscale) at which the formation of magnetic domain walls becomes energetically unfavorable. In such a case, all moments in a particular particle will be aligned in the same direction. Hence every particle is a single domain, acting as a single colossal magnetic moment.

As in paramagnets there will be some temperature at which the constitute particles posses enough energy to rotate freely and align with an external field. Additional, below this temperature the particles will not be able to rotate freely, and are referred to as blocked. This type of magnetic behavior is referred to a superparamagnetism [36]. Many superparamagnets

show behavior that follows a Curie type law but with exceptionally large values for the material specific curie constant.

2.2.6 Spin-glass

Another type of magnetic behavior of great interest is that of a spin-glass. Its magnetic ordering is analogous to the positional ordering of a conventional, chemical glass, hence the term "spin-glass" [37]. The net magnetization (in the absence of an external field) is effectively zero, as in a paramagnet.

A spin glass (in the absence of an external magnetic field) posses no ordering as in a paramagnet, except that instead of the dipole's dynamic disorder, there a static frustrated interaction disorder (like a glass). This particular type of ordering is usually referred to as a "frozen in" disorder, as opposed to the dynamic disorder in a paramagnet (in the absence of an external magnetic field).

2.2.7 Superspin-glass

Analogous to the relationship of a superparamagnet to a paramagnet, is that of a super spin-glass to a spin-glass. The super spin-glass behavior is basically defined identical to that of a spin-glass, the only difference being what are considered the constitute particles.

In a super spin-glass the composite particle are considered single domain ferromagnetic nanoclusters, while in a regular spin-glass they are just the atomic dipoles. Physically the behavior of a super spin-glass is attributed to the nanoparticles being densely packed within the material [38].

2.3 Magnetic Behavior

We can generally express a particular type of magnetic transition in terms of energy barriers/constraints. If enough excess energy (typically thermal) is supplied to the material it

could effectively overcome or nullify these barriers/constraints, and the material would then exhibit a new type of magnetic behavior. Essentially we have material specific magnetic transitions, and corresponding transition temperatures.

There are numerous theories involved with these magnetic phases and magnetic phase transitions. Usually a good indicator of a particular magnetic system/transition is that the data can be fit to a corresponding mathematical model, although alone this is not enough to confirm a particular type of magnetic system. While there are numerous transition models, in this investigation we only touch on the most basic and pertinent to our particular system.

Within all magnetic transition/behavior models, there are a few inherit things that remain constant. Fundamentally magnetic phase transition temperatures correspond to critical points in the magnetization data (susceptibility for example) as a function of energy (i.e. temperature).

2.3.1 Curie and Néel points

In addition to the "effect of distance" overcoming dipoles ability to all align in parallel (in a ferromagnet), "thermal oscillation" or "entropy" may do the same thing. Enough thermal energy may be sufficient to overcome the coupling forces of the ferromagnet. So, in a practical sense, you can say "temperature" is responsible (as an increase in temperature produces increased thermal oscillation and increased entropy).

Up until a certain temperature, a ferromagnet usually has a spontaneous symmetry and often random domains continuously forming and breaking (in the absence of an external magnetic field). Above a critical temperature, the Curie temperature (from Pierre Curie), the material no longer exhibits this spontaneous magnetization, but if you apply an external magnetic field all its dipoles will still align to form a net magnetization, hence it becomes a paramagnet.

Analogous to the Curie temperature for ferromagnets is the Néel Temperature (from Louis Néel) for antiferromagnets, the temperature at which an antiferromagnet becomes a paramagnet.

2.3.2 Curie Law

We mention the Curie law only in passing because it was perhaps the first law developed that accurately described a magnetic behavior. Experimentally discovered by Nobel laureate Pierre Curie through data fitting, the Law relates the magnetic moment of a paramagnetic material to the external magnetic field and temperature of the material [39]. The law is only valid at high temperatures and in the case of weak magnetic fields, as at low temperatures or strong magnetic fields, magnetization saturates.

In its simplest form Curie's law describes the magnetization of a paramagnetic material as being directly proportional to the materials magnetic susceptibility, curie constant, applied magnetic field, and inversely proportional to the temperature.

$$\boldsymbol{M = \chi * H = C * (H / T)} \tag{2}$$

Where $\boldsymbol{M}$ is the resulting magnetization, $\boldsymbol{\chi}$ is the magnetic susceptibility (degree of magnetization of the material in response to the applied magnetic field), $\boldsymbol{H}$ is the auxiliary magnetic field, measured in amperes/meter, $\boldsymbol{T}$ is absolute temperature, measured in Kelvin, and $\boldsymbol{C}$ is a material-specific Curie constant

Note that at some point, increasing the external field will not increase the total magnetization as there is total alignment of the ions already.

2.3.3 Néel-Brown

An important theory to mention when dealing with particles that exhibit superparamagnetism is Néel-Brown Theory. The theory was first developed by French physicist Louis Néel [40] and later refined by American physicist William Brown [41]. The model

essentially describes thermally activated magnetization reversal. The theory explains the magnetic response of single-domain ferromagnets. Since the particles are a single domain, each particle acts as a single colossal magnetic moment.

The anisotropy energy is defined as the energy required to change the direction of magnetization of these moments, and depends on the materials properties as well as size of the particles. As the size decreases, logically so does the energy required to move these particles, and subsequently the temperature at which the material becomes superparamagnetic.

The Néel-Arrhenius equation is used extensively when dealing with superparamagnetic transitions, as well as systems with similar types of relaxations. The equation takes the form of an Arrhenius equation (after Savnte Arrhenius), a particular type of equations originally used to model rates of chemical reactions, hence the name Néel-Arrhenius. The Néel-Arrhenius equation describes a collection of non-interacting nanoparticles with random magnetic direction. The law relates the rate at which particles relax relative to temperature, time and some material specific properties.

The primary equation (Néel-Arrhenius) states that when an external magnetic field is applied for a long time to a superparamagnet and removed, the ferromagnetic clusters will not randomize direction instantly, rather it will take some finite length of time (fraction of a second to years). The size of the clusters then becomes important as larger clusters would need larger energy to move, hence they would hold there magnetization for longer/randomize slower. The simplest form of the Néel-Arrhenius equation is of the form:

$$\boldsymbol{\tau = \tau_0 \exp(E / (k_B T))} \tag{3}$$

where $\boldsymbol{\tau}$ is the average length of time that it takes for a ferromagnetic cluster to randomly flip directions as a result of thermal fluctuations, $\boldsymbol{\tau_0}$ is a length of time, characteristic of the material,

called the *attempt time* (generally on the order of 10^{-9} – 10^{-12} s), **E** is the *magnetic anisotropy energy*, the energy barrier associated with the magnetization moving from its initial "easy axis" direction, through a "hard axis", ending at another easy axis. **E** is directly proportional to a material specific anisotropy constant and particle size, $\mathbf{k_B}$ is the Boltzmann constant, and **T** is the temperature

Above a certain temperature, enough thermal is present to allow the nanoparticles to readily align with an external applied field. In this state the material acts like a paramagnet with giant moments, hence the term *superparamagnet*. However, below this critical temperature (known as the blocking temperature T_B), the lack of thermal energy causes the particles to be unresponsive to a magnetic field within the timeframe of the experiment, and are considered to be blocked.

2.3.4 Vogel-Fulcher

Similarly to the Néel-Arrhenius equation is the Vogel-Fulcher (VF) equation [42,43]. This use was proposed by Shtrikman and Wohlfarth [44] as an alternative law to describe a type of magnetic relaxation system, and by Tholence [45] as a way to describe spin glass relaxations.

Theoretically the main difference between this law and the Néel-Arrhenius law**,** is that this law accounts for some slight inter-particle interactions. The law describes what appears to be a “slowing down” of relaxation processes associated with many spin-glasses. Interesting to note, while the VF equation has been confirmed experimentally to model many types of systems (supercooled organic liquids, spin glasses, polymers), there is still no widely accepted derivation of the law from first principals to a mesoscopic level. The simplest form of the Vogel-Fulcher equation is of the form

$$\tau = \tau_0 \exp(E / (k_B(T-T_0))) \quad (4)$$

where $\boldsymbol{\tau}$ is the average length of time that it takes for a ferromagnetic cluster to randomly flip directions as a result of thermal fluctuations, $\boldsymbol{\tau_0}$ is a length of time, characteristic of the material, called the *attempt time*, **E** is the magnetic anisotropy energy, the energy barrier associated with the magnetization moving from its initial "easy axis" direction, through a "hard axis", ending at another easy axis. **E** is directly proportional to a material specific anisotropy constant and particle size, $\mathbf{k_B}$ is the Boltzmann constant, **T** is the temperature, and $\mathbf{T_0}$ is material specific characteristic temperature that accounts for inter-particle interactions.

2.3.5 Critical Phenomena

Yet another way to describe magnetic relaxation is though critical phenomena behavior. First introduced by Ferrell [46], and later generalized by Hohenberg and Halperin [47], this type of procedure has been known to accurately model many different relaxation systems including superspin-glasses. Mathematically this model accounts for an exponential modeled critical slowing down of the relaxation mechanism. Often this model is used to describe the “slowing down” behavior of the relaxation in collective spin-glass systems above the freezing temperature [48].

This model is used for systems in which anomalous behavior is expected around some critical point, hence the term “critical phenomena”. The region around this point is usually termed the “critical region”. While the full theory behind this type of system is beyond the scope of this investigation, we present a few key points through their application to magnetic transitions.

It is well established that critical points in magnetic data correspond to magnetic phase transitions. For a magnetic system, the order parameter in the phase transition classification scheme is usually the magnetization “M” and the derivative is the susceptibility “χ”. A system

with a second order phase transition (like magnetic phase transitions), is characterized by a discontinuity of the derivative of the order parameter [49]. It therefore makes logical sense that magnetic materials show anomalous behavior around magnetic transition temperatures, "critical phenomena". At these temperatures different magnetic observables should diverge or vanish, based on their relation to the order parameter.

Usually a reduced temperature parameter "ε", $\varepsilon = (1-T/T_F)$, is introduced to account for the change around the transition temperature. In addition we define the correlation length. The correlation length is a parameter that deals with the "average magnetic domain size". The precise physical definition of correlation length is usually defined in terms of spin, through a spatial correlation function Γ(r,T). Γ(r,T) being the probability that a spin at a distance r from a given spin in a particular domain (at equilibrium and temperature T) belongs to the same domain as that spin. Γ(r,T) then varies as $e^{-r/\xi}$, as r approaches infinity [50]. With this relationship, we solve for the correlation length in terms of Γ(r,T) in the limits of r. Albeit that this physical meaning is not as intuitive as other variables in many magnetic modeling theories, this definition is the theoretical standard used. The correlation length is further interpreted (purely for later fitting purposes) solely through the dynamic scaling hypothesis.

In the critical region and the thermodynamic limit, parameters such as correlation length, susceptibility, and time should diverge, while magnetization should vanish, proportionally to the value of the reduced temperature to the corresponding dynamic exponent. Hence for the correlation length:

$$\boldsymbol{\xi = (T/T_F - 1)^{-\nu}} \tag{5}$$

where ξ is the *correlation length*, ν is the *critical exponent* of the correlation length, **T** is the temperature, $\mathbf{T_F}$ is the material specific zero field freezing temperature. This equation is often

referred to as the "static scaling hypothesis". From this equation, we obtain the power law of the form:

$$\tau = \tau_0(T/T_F - 1)^{-zv} \quad (6)$$

where zv is the dynamic critical exponent, T_F is the transition temperature, and τ_0 is a characteristic time constant for relaxation.

This power-law is implored for data fitting, in manners similar to the Néel-Arrhenius and Vogel-Fulcher equations. In addition, various similar equations can be obtained from the critical phenomena behavior, based of the other magnetic observables.

Chapter 3: Experimental Methodology

3.1 Powder X-Ray Diffraction

Powder x-ray diffraction (PXRD) measurements can be taken to determine the chemical structure, phase, and average particle size of a powder sample. A nano-powder sample is essential made up of multiple nano-scale crystals. Ideally a nano-powder sample has enough crystals such that orientation should be represented equally. An x-ray beam is sent directly through the sample producing an expanding cone (Debye-Scherrer) radially outward from the sample at every angle (2θ). Subsequently a 2-d pattern is collected by a flat panel detector on the side opposite the x-ray beam, made up of concentric rings of varying intensity. Taken Bragg's law into account each ring corresponds to a particular reciprocal lattice vector G in the sample crystal.

$$\mathbf{G = q = 2\ k\ Sin[\theta] = 4\ \pi\ Sin[\theta] / \lambda} \tag{7}$$

This data is then integrated angularly and given as a function of angle (2θ), and normalized. It is this new data (intensity as a function of 2θ) that is further manipulated to find the structure of the sample. Due to the tediousness involved in the data analysis process, most x-ray diffraction analysis is done with the aid of advanced computer software.

In addition, database comparisons are often used in powder-x-ray diffraction analysis. Often data is compared to that in a database with already known structures, such as the International Centre for Diffraction Data's Powder Diffraction File [51] and The Cambridge Structural Database [52]. In very extensive databases it may be possible to find an exact match or at least a similar structure to help aid in further analysis.

3.1.1 Geometrical structure

The first information usually obtained though powder x-ray diffraction is the geometric structure of the material. The space group and corresponding lattice parameters are then found through a process known as “indexing”, which involves the positions of the peaks and reflection points of the intensity as a function of two theta [53]. Indexing essentially finds the coordinate structure of the material, but not the particular types of atoms at these coordinates.

3.1.2 Physical substance

After indexing, various “refinement” techniques, based on the relative values of peak intensities, are used to find the types of atoms in the structure. The most common used refinement technique in powder x-ray diffraction is the Rietveld refinement [54]. The Rietveld refinement uses a least square approach to refine a set of theoretical data to the actual data. Once the theoretical data is within a desired similarity to the actual data, the atoms/structure that generated the theoretical data is said to be that of the actual data.

3.1.3 Average particle size

Powder X-ray diffraction data is also often used to calculate the average particle size of a nanoparticle sample. Using the Debye-Scherrer formula it is possible to determine the average nanoparticle size. The Debye-Scherrer formula relates average nanoparticle size to the width of prominent intensity peaks (as intensity is measured as a function of two theta), the shape factor (a constant based of the geometry of the particles), and the wavelength of the incident X-rays [55].

3.2 Magnetometry

Originally the term magnetometer, first coined by Carl Friedrich Gauss as “magnometer”, was an instrument for measuring the earth’s magnetic field [56]. The more modern definition of

magnetometer encompasses any scientific instrument that is used for measuring magnetic fields. Magnetometry is the application and study of advanced scientific techniques used to measure magnetization and magnetic related properties, be it under normal conditions (room temp, no external field), or in more extreme cases (external magnetic fields, changes in temperature, pressure, etc).

There are two basic categories of magnetometry used by scientists in active materials research today, DC Magnetometry and AC Magnetometry. While there are numerous theories and procedures used in magnetometry, the most pertinent to our investigation are those dealing with the identification and distinction between materials with superparamagnetic and super-spin glass behaviors.

3.2.1 DC Magnetometry

By taking a sample (usually with some inherent magnetic properties) and applying a constant DC magnetic field to it, a DC Magnetic Moment of the sample can be measured by inductive techniques, producing the DC M(H) magnetization curve. Although the inductive techniques can vary, the standard is that of moving the sample relative to a set of pick-up coils. The voltage induced on these pick-up coils by moving the sample is what is actually being "measured". It is through calculation of this voltage that the DC magnetic moment of the sample is determined using electromagnetic principles. Practically it can be said that DC magnetic measurements of a sample determines the "equilibrium" value of the magnetization of the sample.

There are two basic protocols for measuring the temperature dependence of the DC Magnetic susceptibility. These protocols are referred to a zero-field-cooled (ZFC) and field-cooled (FC) measurements. In both ZFC and FC, the sample is cooled to some minimum

temperature, and the magnetization measured upon warming. The difference between ZFC and FC is that in FC measurements a magnetic field is applied prior to the cooling of the sample to the minimum temperature, while in ZFC experiments the sample is cooled in the absence of a field.

Generally, DC Magnetometry is used to define magnetic behavior transitions of a sample, as they usually correspond to peaks in the M(T) curve. By overlaying ZFC and FC curves, DC Magnetometry is also used to find the magnetic reversibility/irreversibility behavior of a sample. The reversibility can be seen as convergent curves, and irreversibility as divergent curves.

3.2.1.1 Magnetization as a function of applied field

Measurements of the magnetization of a sample "M" as a function of applied magnetic field "H" provides a plethora of useful information. The initial behavior of magnetization as a function of applied magnetic field can be indicative of the type of magnetic material present. In addition the "magnetic saturation" can be obtained from the final behavior of M. Furthermore, Magnetic M(H) hysteresis information can usually be obtained through some time varied applied magnetic field "H" protocol. Comparisons of M(H) at different scales of a material compound may provide evidence of size dependent magnetic behavior.

The initial behavior of the magnetization as a function of applied magnetic field can be used to differentiate between types of magnetic behavior. A material will usually exhibit a linear relationship between M and H if the composite particles are acting paramagnetically and an exponential relationship if they are acting ferromagnetically or spin-glass like.

If a flattening of the M(H) curve is observed (i.e. M becomes constant with increasing H), then magnetic saturation has occurred. Magnetic saturation occurs when the composite magnetic particles all line up parallel to the applied magnetic field. Naturally once all composite magnetic

particles are parallel to the field, increasing the external magnetic field does nothing to their orientation, and subsequently nothing to the net magnetization of the sample. At magnetic saturation the material is said to be reach a maximum magnetization σ_{max}. While magnetic saturation can be observed in many magnetic systems, there are those (often magnetic nanoparticles) that don't seem to experience magnetic saturation (within the H fields available in a laboratory setting and without destroying the particles).

The hysteresis of magnetization curve M(H) may be measured, by first increasing the H field in steady increments up to some maximum (usually saturation), and then decreasing it in steady increments back to its initial value. The corresponding hysteresis has a variety of parameters associated with it. The coercivity for example is a parameter related to the materials ability to retain magnetization. It is important to note that not all magnetic materials exhibit a magnetic related hysteresis.

Often comparison of magnetization M(H) curves between different scales of a particular chemical system is done initially to determine if size depend magnetic behavior exist. If the magnetization dependence on applied filed is different for different scales, then obviously size dependent behavior exists, and further magnetic properties are then usually investigated. Often size dependent magnetic properties are themselves indicative of specific magnetic systems, notably magnetic nanoparticles.

3.2.1.2 Magnetization as a function of temperature

Zero-field-cooled measurement of the magnetization of the sample as a function of temperature gives rough information about the samples magnetic phase transitions. Further information about magnetic behavior is obtained by the comparison of the field-cooled (FC) and

zero-field-cooled (ZFC) magnetization versus temperature, as well as through associated magnetic memory measurements (TRM).

Essentially the onset of magnetic phase transitions can be observed as the local maxima of the M(T) curves. The corresponding temperatures are called magnetic transition temperatures, and are associated with the onset of magnetic phase transitions. In addition, comparisons of the field-cooled magnetization curve $M_{FC}(T)$, and zero-field cooled magnetization curve $M_{ZFC}(T)$ provide evidence of magnetic phase transitions as well. There are two possible types of observations: 1) $M_{ZFC}(T)$ and $M_{FC}(T)$ curves coincide, magnetic reversibility, 2) $M_{ZFC}(T)$ and $M_{FC}(T)$ curves differ, magnetic irreversibility. Simply put, a material can retain its memory of being in a particular magnetic field, if the sample is cooled is such a way that this magnetic imprint (behavior) is frozen into the structure. Magnetic reversibility implies the system experiences no magnetic related memory, and irreversibility implying the system does experience a magnetic related memory. As some types of magnetic materials exhibit magnetic memory and some do not, reversibility and irreversibility can be indicative of a specific type of magnetic material present within a sample.

In addition, information regarding the thermo-remnant magnetic (TRM) behavior of a sample can be taken by measuring M(T), with some additional time related protocol. Thermo-remnant magnetization deals with a material's magnetic memory imprinting as a function of temperature and time. Thermo-remnant magnetization is commonly used to provide information about the magnetic field of the earth at different points in its history, by means of the frozen in magnetic structure of some ingenuous rocks. Magnetic memory information of a material sample can also provide information about the particular types of magnetic systems within the sample.

Thermo-remnant magnetization measurements of a material are typically carried out in a two-step process. 1) In a constant magnetic field, the sample is quenched from some "final temperature" above the transition temperature (quenching may be continuous or involve a "stop-wait" protocol) to some "initial temperature". 2) The magnetic field is then removed and the material is heated up at a constant rate back to the "final temperature". As the material is heated magnetization measurements are made as a function of temperature.

Thermo-remnant magnetization behavior involves a "reference" measurement and "actual" measurement. The "reference measurement" is when the material is quenched continuously, whereas "actual measurements" involve a "stop-wait" quenching protocol. The "stop-wait" quenching involves the sample being quenched until a certain "intermediate temperature", at which point it "waits" for some given amount of time. After the "wait" the sample is further quenched down to the "initial temperature". The difference between the "actual" and "reference" M(T) curves indicates behavior that can be directly related to a specific type of magnetic system.

3.2.2 AC Magnetometry

Just as in the DC Magnetometry, AC Magnetometry involves a sample (usually with some inherit magnetic properties), in a constant DC magnetic field. The difference is that with AC Magnetometry you add a small AC magnetic field to the constant DC magnetic field. The resultant superimposed field, ends up having time dependence (because the AC field has time dependence). Due to basic electromagnetic principles, the magnetic moment of the sample in the field ends up producing a current in the induction coils as well. The new "moment" produced by the superimposed field, can be called the AC magnetic moment, which is time dependent [57].

At low frequencies, the induced AC Magnetic moment depends on the change in DC magnetic moment M(H) (in response to the AC field), as well as the phase and amplitude of the AC field. Naturally as the AC field approaches zero, the AC magnetization curve becomes the DC magnetization curve. This behavior is standardly written as follows:

$$M_{AC} = \chi * H_{AC} \text{ Sine}(\omega t,) \quad (8)$$

where M_{AC} is the induced AC Magnetic Moment, H_{AC} is the amplitude of the driving field, ω is the driving frequency AC field frequency, and $\chi = dM/dH$ is the slope of the $M(H)$ curve, called the AC susceptibility, and is usually the quantity of interest in AC Magnetometry.

In cases of high frequency, the magnetization of the sample may end up lagging the AC field (concluded from the principles of electromagnetics), we therefore end up with two components for the AC susceptibility, a magnitude χ and a calculated phase shift φ (relative to the driving signal). Alternatively (using basic trigonometry) you can think of the AC susceptibility as having a real or in-phase part χ' and an imaginary or out-of phase part χ'' (computed from the phase and magnitude).

$$\chi' = \chi \, Cosine(\varphi) \quad (9)$$

$$\chi = (\chi'^2 + \chi''^2)^{1/2} \quad (10)$$

$$\chi'' = \chi \, Sine(\varphi) \quad (11)$$

$$\varphi = ArcTan(\chi''/\chi') \quad (12)$$

Both the real part and imaginary parts of AC susceptibly are extremely sensitive to thermodynamic phase changes, and are therefore key instruments in measuring transition temperatures.

AC magnetometry allows one to probe all sorts of interesting magnetic phenomena. Typical measurements performed are harmonic measurements, χ (real and imaginary) vs.

temperature, driving frequency, DC field bias, and AC field amplitude. AC magnetometry measurement data is usually taken to be fit to some particular magnetic model (Néel-Brown, dynamics scaling, etc). If the data is found to fit some particular model relatively well and DC magnetometry measurements confirm this, then naturally the underlining physics that implied the model is taken as the underlying physics of the material.

3.2.2.1 AC susceptibility varying frequency

AC susceptibility measurements taken as a function of temperature while varying AC field frequency can be a strong indicator of a particular type of magnetic behavior. Magnetic transition temperatures usually correspond to susceptibility maxima, for some particular applied AC field frequency. Through variation of the AC field frequency, a single observed magnetic transition can produce multiple magnetic transition temperatures. With a good amount of transition temperatures and corresponding AC field frequencies, this data is fitted to a corresponding magnetic transition model (Néel-Brown, Power Law,…etc) each indicative of a particular type of magnetic behavior. It is then possible to extrapolate the zero-field magnetic transition temperature, DC transition temperature, from the particular magnetic model. In addition relative variation of the peak temperature per frequency decade may be measured from the transition temperature data. The found value of the peak temperature per frequency decade being indicative of a particular magnetic system.

Within each particular magnetic model there are some parameters that are to be solved for by data fitting (given a good amount of transition and frequency data). Once these parameters are solved for they are checked for physical sense, i.e. the parameters make sense physically. In addition these parameters are checked to be in some established range for the particular magnetic model. If there parameters make physical sense and are in range, there is a strong indication that

the material present in the sample is that described in the particular magnetic model (paramagnetic, spinglass, etc).

Another calculation that usually accompanies AC susceptibility measurement, as a function of temperature, is the relative variation of the peak temperature per frequency decade. The relative variation of peak temperature per frequency decade is commonly found through the relation:

$$\mathbf{k = (\Delta T / (T\, \Delta log[\omega]))_{ave}} \quad (13)$$

where **ω** is the angular frequency corresponding to the AC frequency of the applied H field, **T** is the average of all magnetic transition temperatures for the particular magnetic transition, **ΔT** is the difference of two successive magnetic transition temperatures, **Δlog[ω]** is the difference of the logarithms of the two corresponding successive angular frequencies. The magnitude of **k** is usually indicative of a certain type of magnetic transition system.

3.2.2.2 AC susceptibility varying magnetic field

By taking AC susceptibility as a function of temperature, yet varying applied magnetic field, information about the magnetic behavior of the sample can be obtained. At each particular value of applied magnetic field there is a corresponding magnetic transition temperature, which itself corresponds to maxima in AC susceptibility. With a good amount of transition temperature data, each with a corresponding magnetic field, the behavior of transition temperature as a function of applied field can be deduced. In addition extrapolating this relationship should provide the zero-field transition temperature or the DC transition temperature.

Generally, the transitions temperature dependence of applied field is written as $\delta T_F \alpha H^N$, with $\delta T_F = 1\text{-}T/T_F$, and the exponent N is found by data fitting. In the situation that a particular N cannot be found to fit all data, the data is broken up into several cases (high H, low

H, etc), and then exponents N are found for every case. The amount of cases needed as well as the particular values of the corresponding exponents, are used as strong indicators that the sample fits some particular magnetic behavior.

The theory behind the correlation between $\delta T_F \alpha H^N$ and a particular magnetic behavior comes from the mean-field theory magnetic model of Sherrington-Kirkpatrick [58], as well as its modification by Almeida-Thouless [59] and Parisi [60]. While this model is well beyond the scope of this investigation, basic understanding of several key results is pertinent. Essentially, this model leads to a presumed exact phase diagram of magnetic behaviors, which include the spin-glass, paramagnet, ferromagnet, and mixed phase. The mixed phase is a ferromagnetic phase with replica symmetry breaking, or magnetic "irreversibility". The boundary between the mixed-phase and the ferromagnetic phase is often referred to as the Almeida-Thouless line "AT-line" [37]. The magnetic phase diagram allows for correlation between magnetic phase transitions and the magnetic transition temperature (as a function of magnetic field H).

3.2.2.3 Scaling and Data Collapse

In our analysis of AC magnetometry data, we will implore the process known as "data collapse" in order to determine the "scaling" behavior of our system. Although the theoretical framework behind "scaling" and "data collapse" is vast and for all practice purposes beyond the scope of this investigation, we still include some of the most basic and useful results that arise from these theories. Finite size scaling is an important theoretical framework for understanding and analyzing physical systems that involve diverging length scales. Finite size scaling is commonly used in nuclear, condensed matter, high-energy, equilibrium and non-equilibrium physics (just to name a few). Additionally for many physical systems which show self-similar or

self-affine characteristics, such as in the dynamics of phase transitions, data collapse is a reliable mathematical tool to establish scaling relations and extract the associated exponents [61].

For all intensive purposes, scaling is best defined on a purely mathematical basis. Defining the arbitrary variable m as a function of variables t and L: m(t,L) experiences scaling if it can be expressed as $m(t,L) = L^d f(t/L^c)$. The parameters c and d are commonly referred to as the exponents, and f is referred to as the scaling function. If by chance the variable L is a linear dimension of the system, and t doesn't equal L, the scaling is said to be finite. Scaling has been applied to a multitude of variables and systems, m often referring to magnetization, specific heat, size, width of a growing or fluctuating surface and so on.

Applying scaling to the thermodynamic limit of infinite sized systems, L and t usually represent thermodynamic parameters, usually associated with magnetic field measurement, pressure measurement, chemical potential measurement, or possibly time. The exponential parameters are usually chosen to not represent any physical parameter, but rather as independent variables, whose values are solved by data fitting. More often then not, L is used to represent some length scale, in which case the dimensionally of d and m are the same, and the dimensionally of c and t are the same. In addition, in fluctuation-dominated cases, c and d assume nontrivial values (those not expected from dimensional analysis).

Remarkably though scaling, behavior of many systems can then be categorized simply by the exponents and the scaling function. Furthermore, scaling implies that two completely independent variables (exponents) can combine in nontrivial ways to form a single variable, which in turn simplifies the description of the observed system.

Originally observed by Rushbrooke [62], data collapse is a common method to observe scaling behavior. The basic premise of data collapse states: coexistent curves in simple systems can be made to fall onto a single curve, or "collapse", if plotted property.

The most common way to use data collapse to observe scaling behavior is though direct algebraic manipulation of the scaling definition. The scaling definition leads to the more useful relation, $m(t,L)\ L^{-d} = f(t/L^{c})$. If mL^{-d} is plotted for various t and L, it is then possible to collapse all curves onto the scaling function, by data fitting for values of the exponents. This type of data collapse represents a powerful method for establishing scaling behavior of a system, and is used extensively to analyze and extract exponents.

Scaling and data collapse are known ways to observe different types of parameters in systems involving magnetic transitions. Typically parameters such as susceptibilities, correlation lengths, and relation types have been known to experience scaling behavior around transition temperatures. Through data collapse, the particular values of the exponents found are highly indicative of the type of magnetic systems present within a particular material.

3.3 Magnetic characteristics

The primary goals in our investigation will be to identify the magnetic behavior within our sample. We know that our sample is composed of nanoparticles, hence we initially concern ourselves with magnetic behavior that is known to exist in nanoparticles of similar structure. If we make the assumption (based on similar studies done) that our individual nanoparticles will act as constitute magnetic particles (each a single domain), our magnetic behavior is likely to be ferromagnetic, superparamagnetic, and superspin-glass like. We therefore focus on the magnetometry methods/data that can observe/distinguish between these magnetic behaviors.

3.3.1 Superparamagnetic

The DC ZFC and FC behavior are more or less understood for superparamagnetic systems. An average magnetic transition temperature should be observed at the maximum of the ZFC curve. In superparamagnetic systems there should be bifurcation (splitting of the curves) at the some temperature at or above the ZFC average transition temperature.

Another good indication of superparamagnetic behavior comes from the hysteresis data of DC magnetization as a function of applied field H. There should be an apparent hysteresis, at temperatures below the blocking temperature, and no hysteresis at temperatures above the blocking temperature.

Typically the AC magnetic susceptibility (real and imaginary) is measured as a function of temperature at some defined AC field frequencies. Using the Néel-Brown theory for single domain magnetic particles, one can easily obtain blocking temperatures, as each blocking temperature should correspond to the temperature at the maximum value of real susceptibility (when real susceptibility is plotted as a function of temperature). With a multitude of blocking temperatures (each corresponding to a different AC frequency) there is enough data to be substituted into the Néel-Arrhenius equation (in frequency). Using best fits, it is relatively simple to find values for the magnetic anisotropy energy and attempt frequency

Naturally if the value of the magnetic anisotropy energy and attempt frequency in the Néel-Arrhenius equation cannot be found such that they work for all blocking temperatures and frequencies, the theory has obviously failed. In addition if values are found that are seemingly physically nonsensical (negatives, extremely small or large) the theory has failed as well. In the case of a failed theory, often modification is needed taking into accountinter- particle

interactions, etc. In the extreme case, perhaps the assumption that the system was superparamagnetic was false, and a new theory is needed.

Additionally, it is worth mentioning that in many cases a Vogel-Fulcher law is used in place of the Néel-Arrhenius law regarding superparamagnetic transitions with slight particle interactions. With such a system essentially all methodology will be the same as that previously described, except an addition parameter will need to be fit for. The characteristic temperature will need to be found by data fitting in the same manner that the magnetic anisotropy energy and attempt frequency were found (making the minimum number of data set needed three).

Another confirmation of superparamagnetic behavior can come from observation of the relative variation (per frequency decade) "k" of the peak temperature. The data needed to obtain k is simply a multitude of transition temperatures and corresponding AC field frequencies (the same ones used in the Néel-Arrhenius equation). It has been observed that superparamagnets will present k values typically around or above 0.3.

Yet another confirmation of superparamagnetic behavior comes for the behavior of the blocking temperature as a function of the magnetic field. To obtain this information we must take AC susceptibility measurements as a function of temperature for particular values of the applied DC magnetic field. It is known that for high H, transition temperatures should show a H^2 dependence [59]. Furthermore once the relationship between transition temperature and the H field is known, extrapolation can be done to determine the zero filed transition temperature once again. This is often done as simply another verification to check that consistent results are being obtained.

Additionally, TRM measurements can provide evidence of non-interacting superparamagnetic behavior. The difference between the actual and reference measurements ΔM

$= M_{act} - M_{ref}$ of a superparamagnetic systems should essentially show no prominent peaks of any sort [63].

3.3.2 Superspin-glass

Superspin-glasses and superparamagnets essentially show the same type of behavior in ZFC/FC temperature dependent DC magnetization measurements as well as in field dependent DC magnetization measurements. In a superspin-glass system, an average magnetic freezing temperature should be observed as a maximum in the ZFC, additionally a bifurcation (splitting of the ZFC, FC curves) should be observed at some temperature at or above the freezing temperature. Additionally, the M(H) data should show an apparent hysteresis, at temperatures below the freezing temperature, and no hysteresis above the freezing temperature.

Because superspin-glass is a true phase transition the theory of critical dynamics is often implored in there modeling. Typically AC magnetic susceptibility (real and imaginary) is measured as a function of temperature at some defined AC field frequencies. Freezing temperatures are obtained as they correspond to the temperature at the maximum value of susceptibility. With a multitude of freezing temperatures (each corresponding to a different AC frequency) there is enough data to be substituted into the power law (derived from the theory of critical phenomena).

Using best fits it is relatively simple to find values for the zero field freezing temperature, the dynamic critical exponent and attempt frequency (minimum of only three measurements necessary).

If the parameters in the power law cannot be found such that they work for all freezing temperatures and attempt frequencies, the theory has obviously failed. In addition if values are found that are seemingly physically nonsensical the theory has failed as well. Spin-glass

behavior has typically reported values of the dynamic critical exponent between 8 and 10, and attempt frequency between 10^{11}Hz and 10^{13}Hz [64].

Another confirmation of a spin-glass behavior can come from observation of the relative variation (per frequency decade) "k" of the peak temperature. The data needed to obtain k is simply a multitude of transition temperatures and corresponding AC field frequencies (the same ones used in the Power law equation). It has been observed that classic superspin-glass systems will present values between .007 [65] and 0.05 [66].

Yet another confirmation of superspin-glass behavior comes for the behavior of the freezing temperature as a function of the magnetic field. To obtain this information we can take AC susceptibility measurements as a function of temperature for particular values of the AC magnetic field H. (Note this is different then the data we use in the power law, where was taken varying specific values of AC frequency). For Higher values of H, freezing temperature should show a $H^{2/3}$ dependence (The Almedia-Thouless line), which is a well established indication of a true phase transition [59]. For low values of H, freezing temperature shows a $H^{1/2}$ dependence [67]. Once the relationship between freezing temperature and AC field H is known interpolation can then be done to find the zero-field freezing temperature which should be in agreement with the temperature found using the power law.

Additionally, finding a scaling relation through data collapse is another useful way to test a material for superspin-glass behavior (as this method is applicable to true phase transitions). Temperature dependence of the imaginary AC susceptibility *x''* (at different AC field frequencies *f*) should provide enough information to allow for data collapse to be calculated (if it exists). It is expected that data collapse can be observed when the dynamic critical exponent is taken as exponent c, AC frequency is taken as the parameter t, T/T_F*-1* is taken as parameter L,

T*x'' or x'' is taken as the function m, and exponent d is to be fitted (see scaling and data collapse section for full info). If indeed data collapse is observed and the exponent d is found to be in good agreement with already established results of superspin-glass systems, then this is yet another strong indication of spin-glass behavior [68,69].

Additionally, TRM behavior of a magnetic sample can be indicative of superspin-glass systems. The difference between the actual and reference measurements $\Delta M = M_{act} - M_{ref}$ of a superspin-glass systems should peak at the stop temperature, and show no other type of enhancement (no additional prominent peaks) [63]. This has been explained as the sample retaining a memory of a quasi-equilibrium state after aging in a weak field at the stop temperature. This quasi-equilibrium gets lost upon further quenching, but rediscovered upon heating, do to the chaotic nature of the superspin-glass state [70,71].

Chapter 4: Experimental Procedure

4.1 Sample Preparation

$Ni_{0.5}Zn_{0.5}Fe_2O_4$ nanoparticles were prepared using the co-precipitation method at Centro de Investigation en Materiales Avanzados (CIMAV). $Ni(NO_3)_2 \cdot 6H_2O$, $Zn(NO_3)_2 \cdot 6H2O$ and $FeCl_3 \cdot 6H_2O$ were dissolved into distilled water at room temperature with a NaOH solution added as precipitating agent. A 1-hour digestion step at 90ºC was carried out to crystallize the phases. Eventually, the precipitated particles were thoroughly washed and dried at 60ºC.

4.2 X-ray Diffraction Measurements

Synchrotron X-ray powder diffraction measurements were performed on the X7B beamline at the National Synchrotron Light Source (NSLS), part of Brookhaven National Laboratory. X7B uses a Si(311) grating system, is capable of x-ray energies of 25-50keV and provides around 10^{11} photons per second.

X-rays of wavelength 0.922Å were selected by a double flat-crystal monochromator and a Mar345 flat image plate was used to detect the diffracted beam. Diffraction images were collected using an exposure time of 60 s.

4.3 Magnetic Measurements

Magnetization experiments were carried out using a Quantum Design Physical Property Measurement System (PPMS) at The University of Texas at El Paso, Structural Physical-Property Research Laboratory (Physics Department). The PPMS is able to probe DC magnetization as well as AC susceptibility, using the inductive techniques described in the last chapter. The PPMS delivers temperature resolved magnetic measurements, capable of magnetic fields of 7 Tesla (70 kOe) and temperatures of 2 to 350 Kelvin. Before each set of measurements the magnetometer was calibrated using a palladium standard.

Zero-field cooled and field cooled magnetization “M” measurements were taken from 3K=T=300K, at H=100Oe. The hysteresis information of DC-magnetization “M” as a function of applied magnetic field “H”, was taken for -3 kOe = H = 3 kOe at temperatures T=3, 250 K. The thermo-remnant magnetic (TRM) behavior of the sample was observed by quenching from 200K to 100K. Measurement was taken involving a stop-wait protocol of 9999s at 120 K, in addition to the reference measurement. The real AC susceptibility as a function of temperature was probed at frequencies, .1, .5, 1, 5, 10 kHz, at 3Oe. Furthermore real AC susceptibility as a function of temperature was probed at H magnitudes, 100, 150, 200, 250, 300, 350Oe, at 300Hz.

Chapter 5: Results and Discussion

Powder x-ray diffraction images were processed by integrating over the projections of the Debye-Scherrer cones onto the flat detector (Fig 5.1) using the Plot2D software. All peaks in powder x-ray diffraction data (Fig 5.2) could be indexed to the standard pattern of Ni-Zn ferrite in the International Centre for Diffraction Data's Powder Diffraction File [51] (PDF # 08-0234), implying there were no impurities present in the sample. The structure of the sample is space group Fd-3m with lattice parameter a=8.38Å.

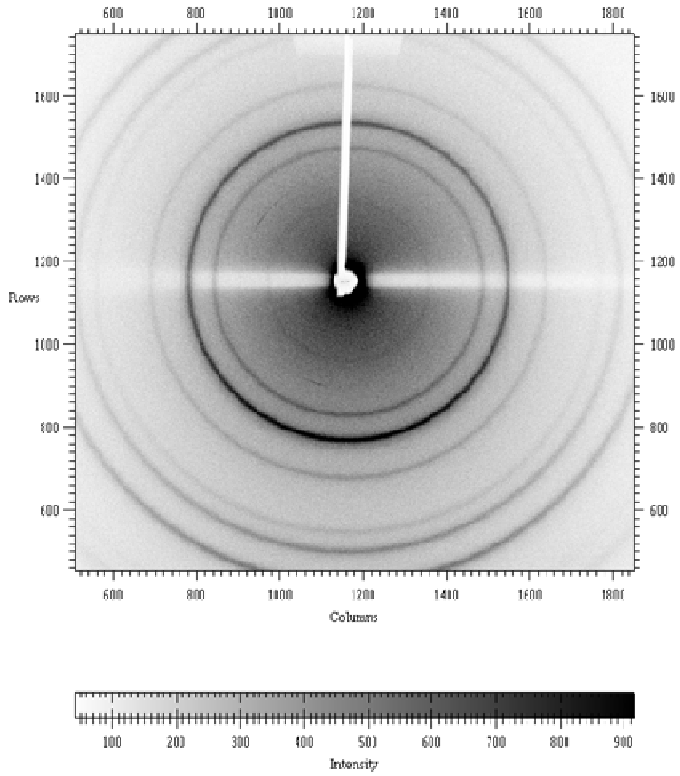

Figure 5.1: Debye-Scherrer cone projection

The full width at half maximum (FWHM) of the (440) peak was obtained from the best fit of the peak profile to a combination of Gaussian and Lorentzian functions

The average nanoparticle size was determined from the full width at half maximum (FWHM) of the (440) peak by means of Scherrer's formula and found to be 9nm (Fig 5.2).

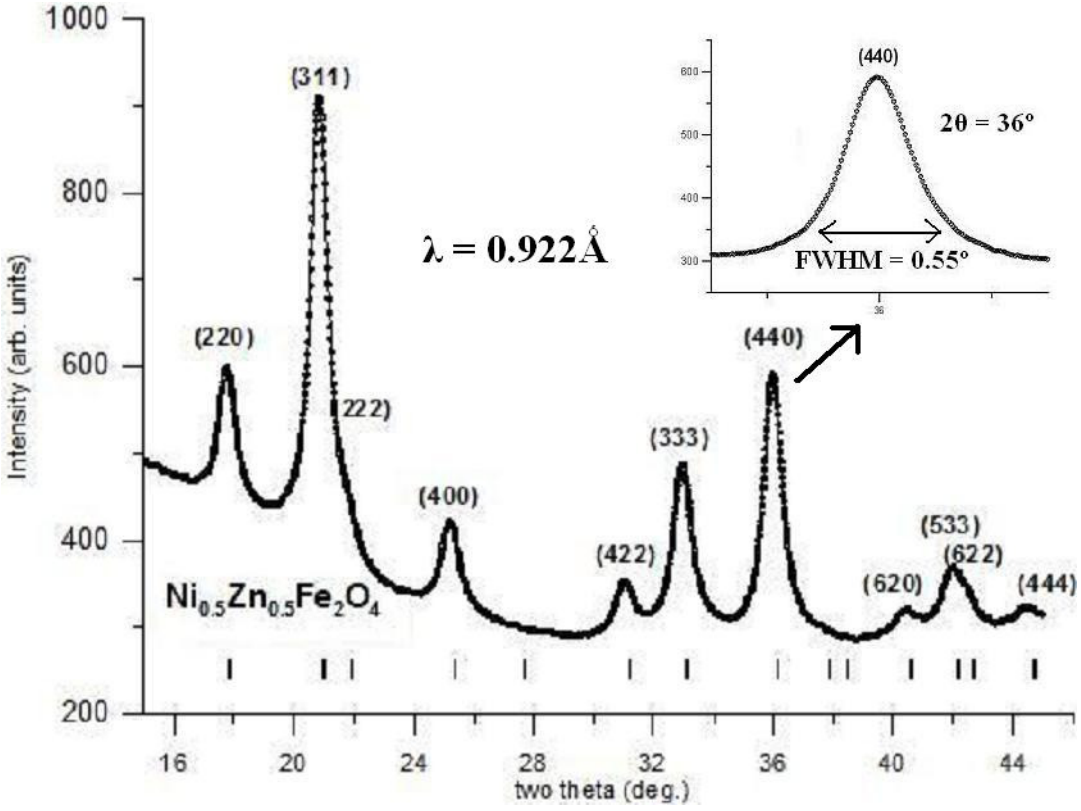

Figure 5.2: I vs 2θ and FWHM

DC Magnetization as a function of temperature showed a bifurcation at 170K, as indicated by the splitting of the zero-field cooled and field cooled data. A magnetic blocking temperature is also observed as the maximum of the ZFC curve at 153K. This is typical of superparamagnetic nanoparticle systems. (Fig. 5.3)

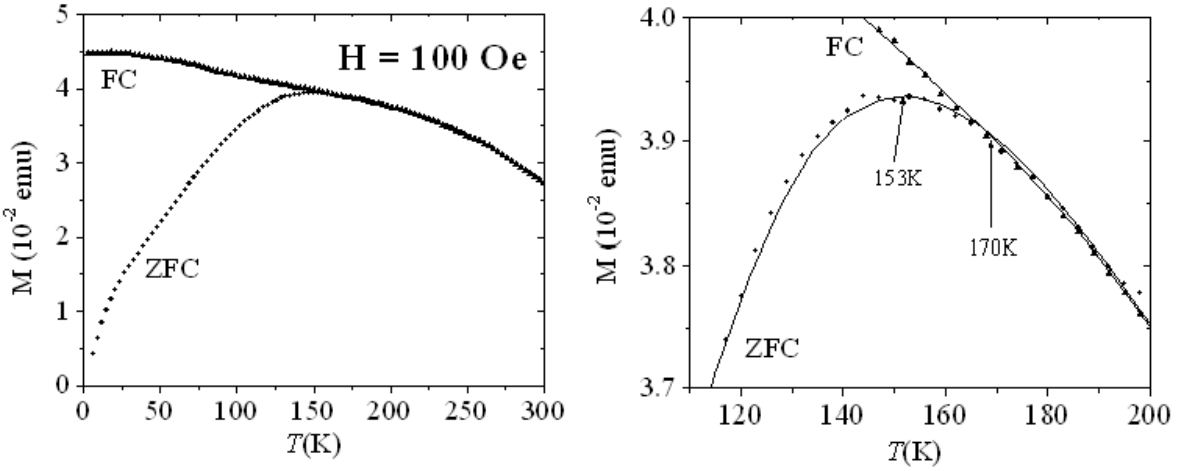

Figure 5.3: M(T), ZFC, FC

M(H) data was further obtained to verify superparamagnetic behavior. The temperature of 3K was picked as it would be well below any thought magnetic transition. Similarly the temperature of 250K was picked as it would be well above the magnetic transition. Hysteresis is exhibited at the 3K curve and not at the 250K (Fig 5.4). This means that the material at 3K is below the blocking temperature while the material at 250K is above the blocking temperature. Again this would be consistent with superparamagnetic behavior.

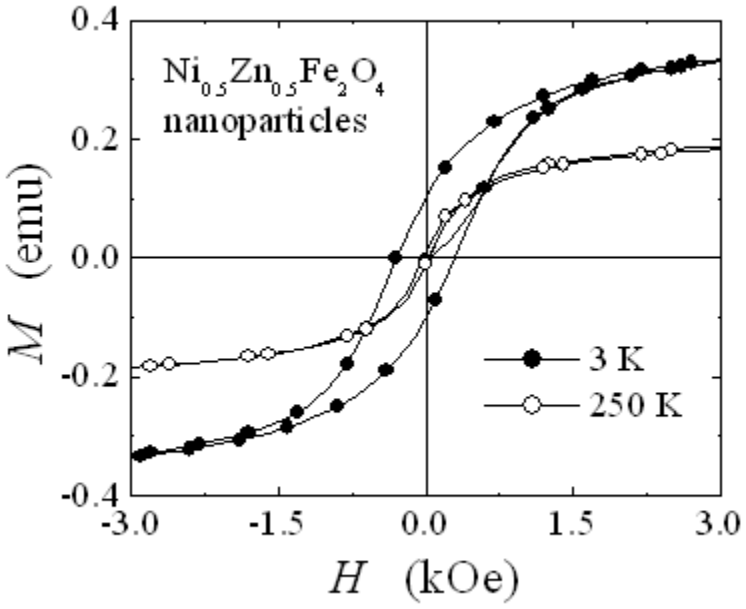

Figure 5.4: M(H), Hysteresis Loop

AC susceptibility data was taken as a function of temperature to further confirm superparamagnetic behavior. Peak temperatures of the real susceptibility at the given AC frequencies were calculated by extrapolation of the data though means of ninth degree polynomial fits. The relative variation per frequency decade was then calculated, it was found to be 0.032 (Fig 5.5). This falls nicely within the range of values observed for spin glass systems (i.e. 0.007 [65] - .05 [66]). We further searched for a magnetic model that account of the observed behavior of the transition temperatures.

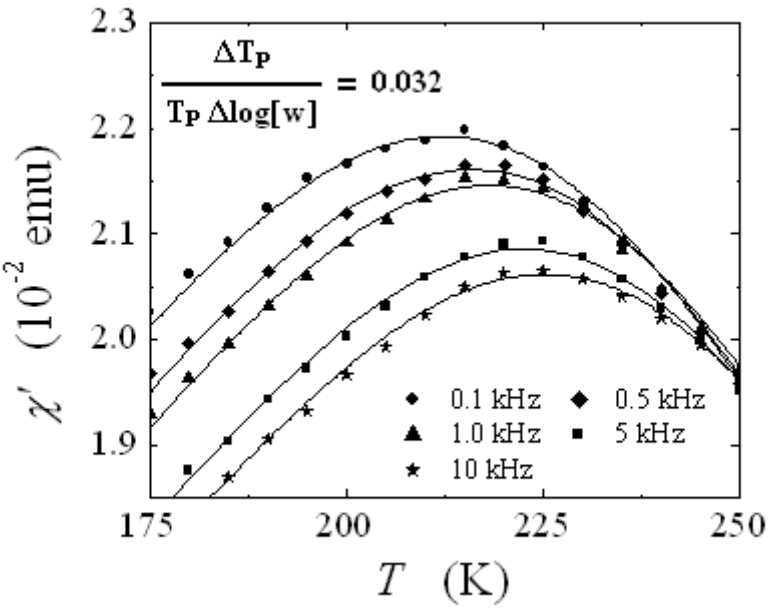

Figure 5.5: AC real susceptibility varying *f*

The Néel-Arrhenius model was initially used but provided unrealistic results for the attempt time and anisotropy energy (Fig 5.6). Data analysis using the Néel-Arrhenius model, provided $\tau_0 = 3.62 * 10^{-37}$ s and $E = 1.48*10^{-3}$eV. This obviously can't be physically correct, due to the unrealistically small value of the attempt time. The Vogel-Fulcher law was then used, providing values of $\tau_0 = 1.07*10^{-9}$ s, $E = 4.48*10^{-2}$eV and T_0=180K. While this fit does describe our behavior reasonably, the Vogel-Fulcher model is a phenomenological model. Consequently, the Vogel-Fulcher fit only suggest that interparticle interactions play a role in the overall behavior of the material.

With the Néel-Arrhenius and Vogel-Fulcher models suggesting that our sample was not strictly superparamagnetic, further investigation was done in attempt to prove the material was super-spin glass like. We decided to examine this possibility because the relative variation per frequency decade is in the superspin-glass range.

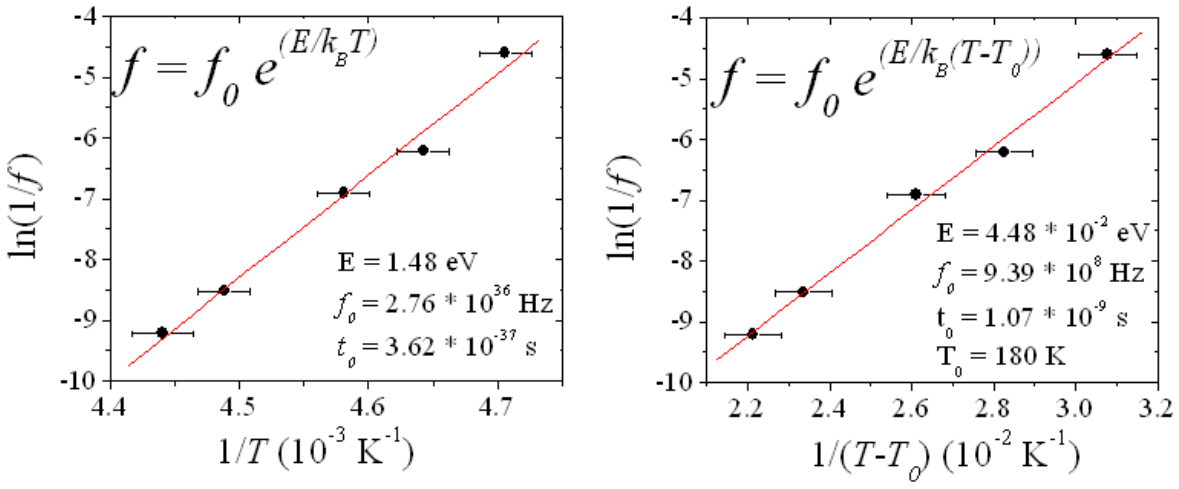

Figure 5.6: Néel-Arrhenius and Vogel-Fulcher fits

Investigation was done using the power law equation (Fig 5.7), which arise from the theory of critical dynamic phenomena. The power law equation, which has been used substantially to model spin-glasses systems previously, gives reasonable values for the dynamic critical exponent zv = 10, attempt frequency 10^{11} Hz, and transition temperature 190 K. There values are in the established range of zv (8 – 10), and the attempt frequency (10^{11}Hz - 10^{13}Hz), which have been observed as spin-glass systems [64]. This is a significant indication of super spin-glass behavior.

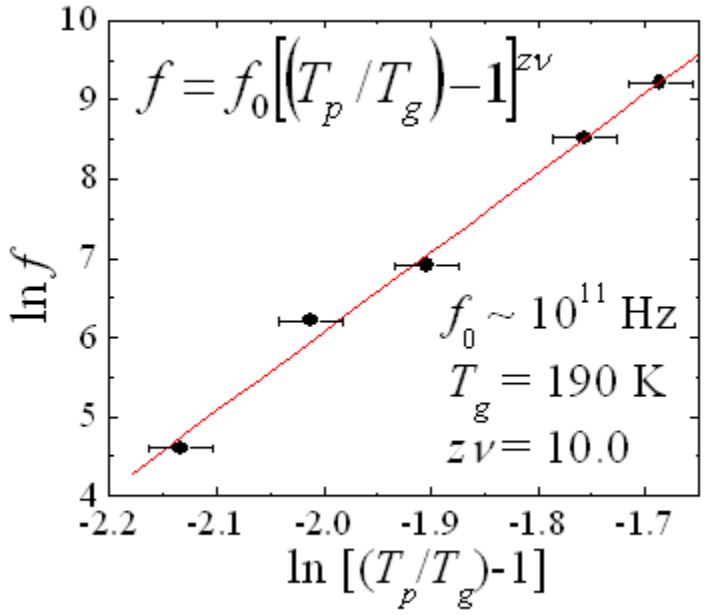

Figure 5.7: Critical Dynamics Power-law fit

Peak temperatures of the real susceptibility at particular H values were found by extrapolation of the data to ninth degree polynomial fits (Fig 5.8). Using these fits, the relationship between peak temperatures and AC magnetic field H was found to be $T_p \alpha H^{3/2}$. Mathematically this implies directly the relationship between δT_F and H is also $\delta T_F \alpha H^{3/2}$. With this relationship known, interpolation can be done to calculate the peak temperature when H=0, the DC transition temperature. Our calculation shows that the DC transition temperature is 190K, which is exactly what we would expect as it is what we observed from our power-law fit. The significant of the exponent 3/2 is referred to as the A-T line, it is known through the Sherrington-Kirkpatrick model [58], and the further modification by Almeida and Thouless [59] that a spin-glass will lie on this line, i.e. $\delta T_F \alpha H^{3/2}$ (Fig 5.9).

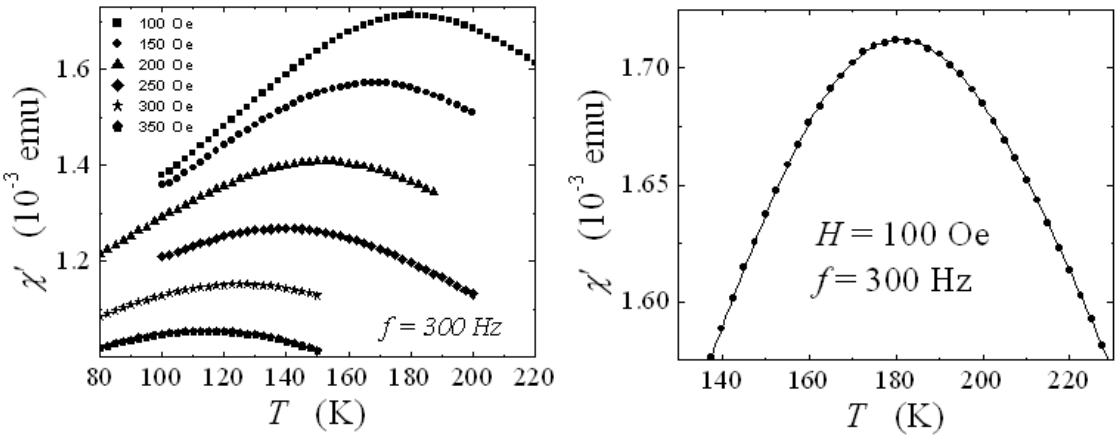

Figure 5.8: AC real susceptibility varying

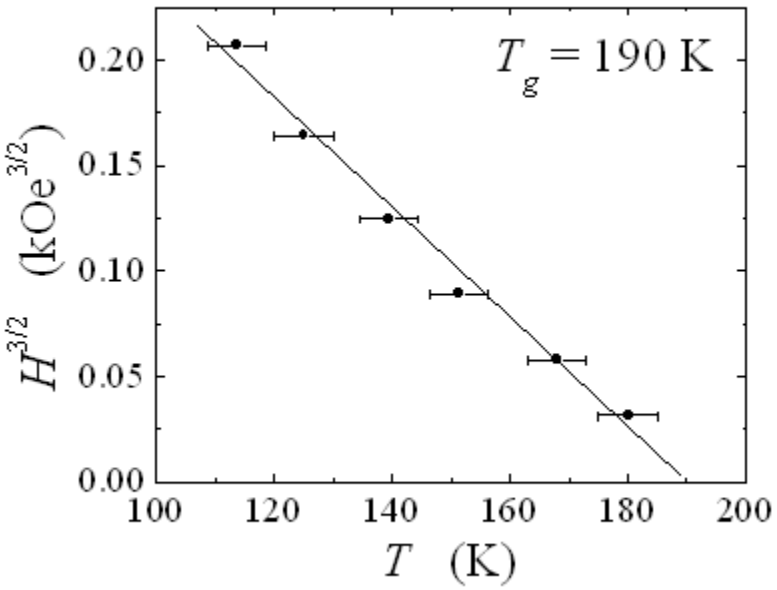

Figure 5.9: Almeida-Thouless line

Further super-spin glass behavior was observed throughout the scaling behavior of the AC imaginary susceptibility. Using the dynamic exponent and freezing temperature found from the power law, as well as the data obtained from imaginary susceptibility as a function of temperature (Fig 5.10), we were further able to probe the imaginary AC susceptibility for scaling behavior. It is an established fact that systems such as spin glasses should exhibit this behavior [68,69]. The easiest way to observe such behavior was through some clever algebraic manipulation and data collapse method as described in the previous chapter. There were two various approach we used to find data collapse, one in which the temperature was included within the collapsing function, and one in which I was not. Both cases show an adequate data collapse observed by setting B=1.0, which excellent agreement with many other spin-glass systems [68].

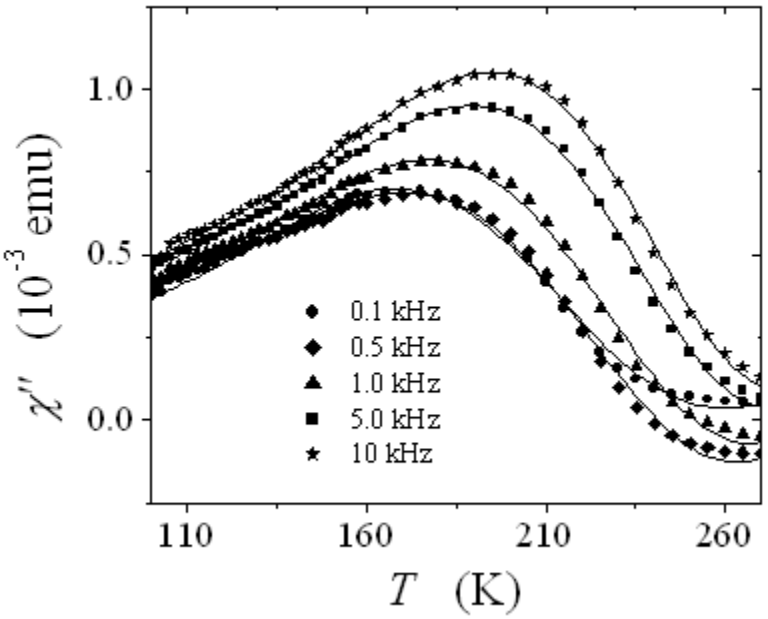

Figure 5.10: AC imaginary susceptibility as a function of temperature

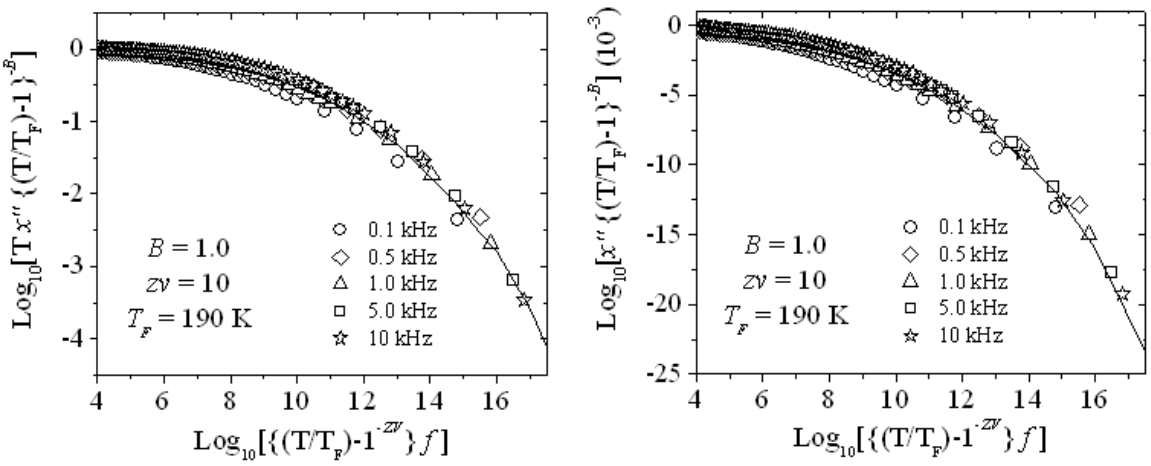

Figure 5.11: Scaling behavior of imaginary susceptibility as shown by data collapse

Our TRM data (fig 5.12) suggest that the material is in fact a super spin-glass, as a peak is observed in ΔM at the stop temperature 120K. A peak in ΔM at the stop temperature is thought be highly indicative of spin-glasses, while absence of a peak is associated with superparamagnetism [63].

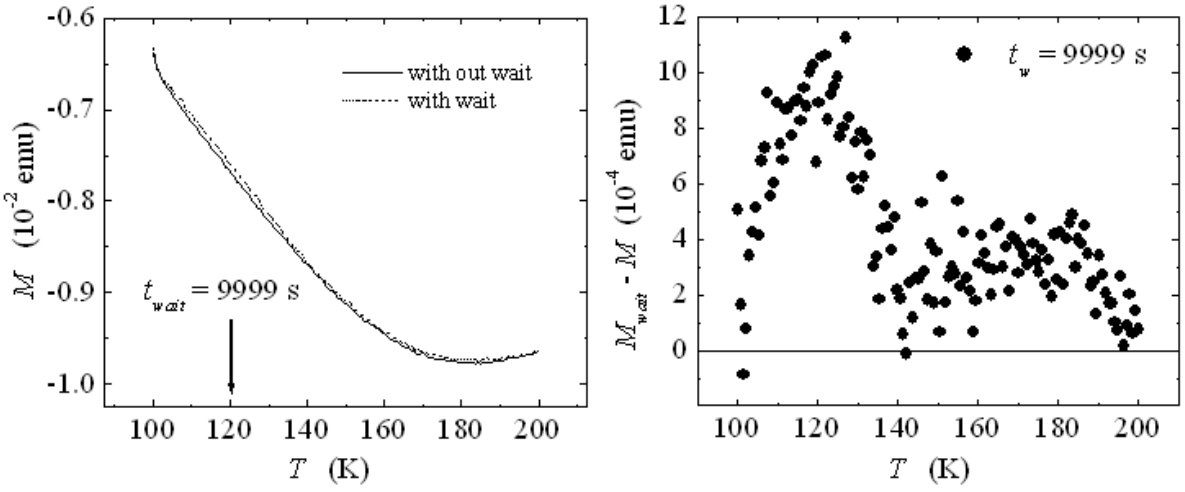

Figure 5.12: Thermo remnant magnetization behavior

Chapter 6: Summary and Conclusions

In our investigation we examined temperature dependent magnetic behavior of nanoparticle $Ni_{0.5}Zn_{0.5}Fe_2O_4$. We used powder X-ray diffraction to determine the average particle size of sample (9nm), as well as to show our sample was impurity free.

Initially our investigation led us to believe that the material would perhaps be superparamagnetic, as ZFC/FC M(T), and M(H) hysteresis data provided result typical of superparamagnets. Upon further investigation of the AC real susceptibility, it was found to be indescribable by the Néel-Arrhenius model (superparamagnetic model) and describable by the Vogel Fulcher equation (typical of particle interactions). Determination of the relative variation per frequency decade suggested that in fact the sample may be a super-spin glass.

Further investigation lead us to conclude that our real AC susceptibility is well described by the power law, a sign of super-spin glass behavior. The transition temperature AC field dependence is found to be on the A-T line and produce an H=0 spin glass freezing temperature consistent with the power law (190K), further super-spin glass behavior. Additionally, dynamic scaling behavior of the imaginary AC susceptibility, yielded best data collapse to parameter B=1.0, which has been shown numerous times for super-spin glasses. Furthermore Thermo remnant magnetization measurements lead to a peak at the wait temperature, this peak has been use previously to differentiate between super-spin glasses and superparamagnets. All apparent data seems to suggest that $Ni_{0.5}Zn_{0.5}Fe_2O_4$ is in fact a superspin-glass and not a superparamagnet.

Chapter 7: References

[1] A. Goldman, *Modern Ferrite Technology*, 2nd ed. (Springer, 2006).

[2] D. Mathew and R.-S. Juang, Chemical Engineering Journal **129** (1), 51-65 (2007).

[3] J. L. Dormann, D. Fiorani and E. Tronc, Adv. Chem. Phys. **98**, 283 (1997).

[4] T. Jonsson and J. Mattsson, Phys. Rev. Lett. **75** (1995).

[5] F. J. Himpsel and J. E. Ortega, Adv. Phys. **47** (1998).

[6] G. A. Prinz and J. H. Hathaway, Phys. Today **48** (1995).

[7] P. Grunberg, Phys. Today **54** (2001).

[8] G. A. Prinz, Science **282**, 1660 (1998).

[9] G. Reiss and A. Hutten, Nature Materials **4**, 725-726 (2005).

[10] A. Ito, Journal of Bioscience and Bioengineering **100** (1), 1-11 (2005).

[11] K. E. Scarberry and E. B. Dickerson, Journal of the American Chemical Society **130** (31), 10258-62 (2008).

[12] P. Nikitin, Sensor Letters **5** (1), 296-299 (2007).

[13] S. X. Wang and A. M. Taratorin, *Magnetic Information Storage Technology*. (Academic, New York, 1999).

[14] S. Sun and C. B. Murray, Science **287** (17) (2000).

[15] J. L. Maurice and J. Briatico, Philos. Mag. A **97** (1999).

[16] (The National Nanotechnology Initiative, 2009)

[17] Y. I. Kim and D. Kim, Physica B **337**, 42-51 (2003).

[18] C. Caizer and M. Popovici, Acta Mater. **51**, 3607-3616 (2003).

[19] D. K. Kim and Y. Zhang, J. Magn. Mater. **225**, 30-36 (2001).

[20] J. A. L. Perez and M. A. L. Quintela, J. Phys. Chem. B **101**, 8045-8047 (1997).

[21] Q. Chen and Z. J. Zhang, Appl. Phys. Lett **73**, 3156-3158 (1998).

[22] Z. X. Tang and K. J. Sorensen, J. Colloid Interface Sci., 38-46 (1991).

[23] C. T. Seip and E. E. Carpenter, IEEE Trans. Magn. **34**, 1111-1113 (1998).

[24] J. F. Hochepied and P. Bonville, J. Phys. Chem. B **104**, 905-912 (2000).

[25] C. Liu and B. Zou, J. Phys. Chem. B **104**, 1141-1145 (200).

[26] E. W. Gorter, Nature **165** (1950).

[27] ASTM Standard E2456, 2003 (2006), "Standard terminology Relating to Nanotechnology," ASTM International, West Conshohocken, PA, 2006, DOI: 10.1520/E2456-06, www.astm.org.

[28] Deer, Howie and Zussman, in *An Introduction to the Rock Forming Minerals* (Longman, 1996), pp. 424-433.

[29] J. K. Burdett and G. L. Prince, J. Am. Chem. Soc., 92-95 (1982).

[30] N. Ashcroft and D. Mermin, *Soild State Physics*. (Harcourt, Orlando, 1976).

[31] M. Massimi, *Pauli's Exclusion Principle*. (Cambridge University Press, 2005).

[32] W. Heisenberg, Magazine of Physics **38** (6), 411-426 (1926).

[33] P. A. M. Dirac, Proceeding of the Royal Society of London A **112** (762), 661-677.

[34] I. Carey, *Magnetic domains and techniques for their observation*. (The English University Press Ltd, London, 1966).

[35] R. Bozorth, *Ferromagnetism*. (IEEE Press, New York, 1993).

[36] C. P. Bean and J. D. Livingston, J. Appl. Phys. **30** (1959).

[37] K. Binder and A. P. Young, Reviews of Modern Physics **58** (4), 801-976 (1986).

[38] P. Jonsson, Adv. Chem. Phys. **128**, 191-192.

[39] P. Curie, School of Physics and Industrial Chemistry at Paris, 1882.

[40] L. Neel, Ann. Geophys. **5** (99) (1949).

[41] W. F. Brown, Phys. Rev. **130** (1963).

[42] H. Vogel, Phys. Z. **22** (1921).

[43] G. S. Fulcher, J. Am. Ceram. Soc. **8** (1925).

[44] S. Shtrikman and E. Wohlfarth, Phys. Lett. A **85**, 467 (1981).

[45] J. L. Tholence, Soild State Comm. **35** (113) (1980).

[46] R. A. Ferrell and N. Menyhard, Phys. Rev. Lett. **18** (1967).

[47] P. C. Hohenberg and B. I. Halperin, Rev. Mod. Phys. **49**, 435-479 (1977).

[48] A. T. Ogielski, Phys. Rev. B. **32** (1985).

[49] L. D. Landau and E. M. Lifshitz, *Statistical Physics*, 3rd ed. (Butterworth-Heinemann, 1980).

[50] M. N. Barber, in *Phase Transitions and Critical Phenomena* (Academic Press, 1983), Vol. 8, pp. 146-268.

[51] (The International center for x-ray diffraction, 2008)

[52] (Cambridge Crystallographic Data Center, 2004).

[53] V. Pecharsky and P. Zavalij, *Fundamentals of Powder Diffraction and Structural Characterization of Materials*, 2nd ed. (Springer, 2008).

[54] H. M. Rietveld, Journal of Applied Crystallography **2**, 65-71 (1969).

[55] A. L. Patterson, Phys. Rev. **56** (10), 978-982 (1939).

[56] C. F. Gauss, Royal Scientific Society **8**, 3-44 (1832).

[57] D. Martien, (Quantum Design Corporation, 2004).

[58] D. Sherrington and S. Kirkpatrick, Phys. Rev. Lett. **35** (26), 1792-1796 (1975).

[59] J. R. L. De'Almedia and D. J. Thouless, J. Phys. A. **11** (1978).

[60] G. Parisi, Phys. Rep. **67** (1980).

[61] J. W. Harris and H. Stocker, in *Handbook of Mathematics and Computational Science* (Springer-Verlag, New York, 1998), pp. 113.

[62] H. E. Stanley, Rev. Mod. Phys. **71** (1999).

[63] K. Jonason and E. Vincent, Phys. Rev. Lett. **81** (1998).

[64] P. Granberg, J. Mattson and P. Nordblad, Phys. Rev. B **44** (1991).

[65] J. L. Tholence and A. Benoit, Soild State Comm. **49** (1984).

[66] J. Ferre and J. Rajchenbach, J. Appl. Phys. **52** (1981).

[67] H. Maletta and W. Zinn, in *Handbook of the Physics and Chemistry of Rear Earths*, edited by K. A. Gschneidner and L. Eyring (1989), Vol. 12.

[68] P. Beauvillian and C. Dupas, Phys. Rev. B. **29** (1986).

[69] T. Zhou and C. Ragaux, Phys. Rev. B. **40** (89).

[70] S. Sahoo, O. Petracic and W. Kleemann, Applied Physics Letters **82** (23) (2003).

[71] J. A. Mydosh, *Spin Glasses*. (Taylor & Francis, 1995).

Chapter 8: Curriculum Vita

Antony H. Adair was born in San Antonio, Texas. He graduated from the Burnham Wood Charter school, in the spring of 2002 and entered The University of Texas at El Paso in the fall of 2003. He graduated from UTEP with a B. S. in Physics and Mathematics in the summer of 2008. He entered the Physics Masters program at UTEP the following semester. As of 2009 he is coauthor of five papers, and has done six conference posters/presentations. He has been a Teaching Assistant since the spring of 2004 for various classes at the UTEP physics department. Antony has been awarded various scholarships, REU'S and internships, including the MARC*USTAR NIH scholarship, an REU at Bringham young university, and an Internship at Northwestern. Antony has worked as an inter computer administer for the Materials research and technology institute (MRTI), as well as traveled to various national laboratories through the MRTI GATEWAY program, including SLAC and LBNL as a user. Antony has been actively involved in the Society of Physics students, and well as UTEP's Math Club (Club Zero). Antony is a member of Sigma Pi Sigma and held the position of president of the Society of Physics students (UTEP chapter) from Spring 08 to Summer 09. In addition Antony was member of the College of Science undergraduate student council, and later the graduate student council, representing both the math and physics department throughout his time at UTEP. Antony will start the PhD program in physics at Rice University in Fall of 2009.

Mailing address: C.O. Physics, 500 West University

El Paso, TX 79968